Article

Discovery Medicine 2025; 37(198): 1243–1262
https://doi.org/10.24976/Discov.Med.202537198.110

Recognizing the Role of Galectin-9 in Chronic Lymphocytic Leukemia: Insights Into Its Combination With Other Disease Parameters to Jointly Determine Chronic Lymphocytic Leukemia Activity

Przemysław Piwowarczyk[1], Agata Szymańska[1], Sylwia Chocholska[2], Michał Zarobkiewicz[1], Justyna Woś[1], Waldemar Tomczak[2], Jacek Roliński[1], Agnieszka Bojarska-Junak[1,*]

[1]Department of Clinical Immunology, Medical University of Lublin, 20-093 Lublin, Poland
[2]Department of Haematooncology and Bone Marrow Transplantation, Medical University of Lublin, 20-080 Lublin, Poland
*Correspondence: agnieszka.bojarska-junak@umlub.pl (Agnieszka Bojarska-Junak)
Published: 20 July 2025

Background: Galectin-9 (Gal-9), a crucial immune checkpoint ligand, plays an essential role in human tumors, but its clinical significance in chronic lymphocytic leukemia (CLL) is still unclear. In the current study, we took a closer look at Gal-9 expression as a part of our quest to identify novel prognostic biomarkers of CLL.

Methods: In this study, 126 untreated CLL patients and 40 age and gender-matched controls were analyzed. Plasma Gal-9 levels were quantified using enzyme-linked immunosorbent assay (ELISA), while Gal-9 expression on immune cells was assessed by multicolor flow cytometry. Confocal microscopy was used to visualize Gal-9 localization on B cell membranes. Epstein-Barr virus (EBV)-miR-BamH1 fragment H rightward facing 1-1 (BHRF1-1) expression was detected via reverse transcription quantitative polymerase chain reaction (RT-qPCR), and digital PCR was used to quantify Gal-9 transcripts in purified $CD19^+$ B cells. The presence of CLL-associated cytogenetic abnormalities was determined by fluorescence in situ hybridization (FISH). The study also identified and characterized B regulatory cell (Breg)-like CLL cells and myeloid-derived suppressor cell (MDSC) subsets (monocytic (M-MDSC), polymorphonuclear (PMN-MDSC), and early-stage (eMDSC)) expressing Gal-9. Survival analyses, including Kaplan-Meier and Cox regression models, were performed to evaluate the prognostic significance of Gal-9 expression.

Results: Our results confirmed an increased expression of Gal-9 mRNA ($p < 0.0001$) as well as an elevated percentage of B-cells with membrane Gal-9 expression ($p = 0.04$) in CLL patients compared to healthy volunteers. Elevated Gal-9 levels in plasma and increased Gal-9 expression on B cells were associated with poor prognostic markers. Notably, the percentage of Gal-9-positive B-cells was found to be an independent prognostic factor of time to first treatment in CLL patients ($p = 0.006$). Plasma levels of Gal-9 were closely linked to the percentages of $CD19^+$/Gal-9^+ ($p < 0.001$), eMDSC/Gal-9^+ ($p < 0.001$), and M-MDSC/Gal-9^+ ($p = 0.001$) cells. Moreover, it was noted that Gal-9 expression was significantly higher ($p < 0.0001$) within the $CD19^+CD5^+CD24^{high}CD38^{high}$ fraction in comparison to the non-Breg CLL cells. Finally, higher levels of Gal-9 expression were linked to EBV positivity and the expression of EBV-miR-BHRF1-1.

Conclusions: Gal-9 expression in leukemic B cells and plasma may serve as a marker of disease activity in CLL. Moreover, an increase in malignant B cell production, along with a boost in MDSC cells, appears to coincide with a significant increase in Gal-9 concentration. Breg-like CLL cells show distinct Gal-9 expression compared to non-Breg CLL cells. Gal-9 may enhance the immunosuppressive potential of Breg. Moreover, EBV-driven Gal-9 upregulation may worsen prognosis in CLL.

Keywords: CLL; Galectin-9; MDSCs; Breg; prognostic markers; EBV; EBV-miR-BHRF1-1; tumor microenvironment

Introduction

Galectins (Gal) are a family of carbohydrate-binding proteins that specifically bind to galactose β-linked to N-acetyl glucosamine [1,2]. Several studies have shown a specific pattern of galectin expression in hematological malignancies [3–5]. Sixteen galectin types exist, with Gal-1, -3, -9, and -12 implicated in leukemia's development and progression [6,7]. Gal-9 can be found in various cellular locations, including the cytosol, nucleus, cell membranes, and extracellular matrix [4,8,9]. It is expressed in numerous cell types, including immune cells like T cells, B cells, natural killer (NK) cells, dendritic cells, macrophages, mast cells, myeloid-derived suppressor cells (MDSCs), and tumor cells [10,11]. In tissues, Gal-9 is located in lymphoid tissues and bone marrow [2,12]. Gal-9 signaling comes through T-cell immunoglobulin and mucin domain 3 (TIM-3) or potentially other receptors such as programmed cell death protein 1 (PD-1), protein disulfide isomerase (PDI),

CD137, CD44, and CD206 [7,13]. Interactions between Gal-9 and its ligand affect immune control, such as cell apoptosis regulation in certain T-cell subsets, promoting Treg differentiation, and influencing macrophage activity [14]. Gal-9 binding to TIM-3 induces Th1 cell death, promotes immune tolerance, and suppresses Th1 and Th17 responses [15]. Intracellular and extracellular Gal-9 promote the expansion and differentiation of MDSCs in the tumor microenvironment [16]. Several clinical studies have elucidated a strong correlation between the expression of Gal-9 and metastasis and recurrence in various solid tumors, such as melanoma, lung cancer, breast cancer, and clear cell renal cell cancer [17–19]. Gal-9 also contributes to the development and progression of various types of leukemia, including acute myeloid leukemia (AML), acute promyelocytic leukemia (APL), adult T cell leukemia (ATLL), and chronic lymphocytic leukemia (CLL) [6,20]. A CLL patient's disease progression and poor prognosis can be linked to a high Gal-9 serum concentration [21,22].

Our most recent findings showed an increase in *Gal-9* mRNA in CLL cells. High levels of *Gal-9* mRNA expression were closely linked with negative prognostic markers [23]. We wanted to confirm these results at the protein level, this time on a much larger group of CLL patients. We investigated the potential role of Gal-9 as a prognostic biomarker in CLL patients by analyzing the level of the soluble form of Gal-9 in plasma using enzyme-linked immunosorbent assay (ELISA) and expression of Gal-9 in B cells using flow cytometry. The results of Gal-9 expression and Gal-9 plasma level analysis were compared with the high-risk factors in CLL. Moreover, despite the extensive study of MDSCs and their role in the CLL microenvironment [22,24,25], there is still little knowledge about Gal-9 expression in MDSCs. Our goal was to assess Gal-9 in MDSC subsets. To the best of our knowledge, we are the first to correlate three MDSC subpopulations, monocytic (M-MDSC), polymorphonuclear (PMN-MDSC), and early-stage (eMDSC) expressing Gal-9 with the plasma concentration of this protein. In addition, we took into consideration that Gal-9 can have an impact on the development of Epstein-Barr virus (EBV) latent infection and the transformation of B cells [26]. Gal-9 aids in the latent infection and lymphomagenesis of EBV in human B cells. It promotes the proliferation of EBV-infected B cells and supports the establishment of latent infection. Additionally, Gal-9 is essential in the regulation of the regulatory function of B cells in patients with CLL, helping to maintain immune tolerance and preventing the activation of autoreactive B cells. Gal-9 acts as an intrinsic regulator of B cell receptor (BCR) signaling and activation [2,27]. In EBV-positive patients with CLL, Gal-9 helps to regulate the activity of B regulatory cells (Breg), ensuring they do not respond to low-affinity self-antigens, which could otherwise lead to autoimmune responses [26]. Therefore, the EBV status of CLL patients was evaluated. Our objective was also to analyze the correlation between Gal-9 and EBV-miR-BamH1 fragment H rightward facing 1-1 (BHRF1-1) expression, which is observed at high levels in B cells undergoing stage III latency [28,29].

Materials and Methods

Study Group

One hundred and twenty-six patients were enrolled in the present study having received a diagnosis of CLL based on the criteria established by the International Workshop on Chronic Lymphocytic Leukemia (IWCLL) [30] and also no history of any other cancer or bone marrow disorder, autoimmune disease, or failure of the circulatory and/or pulmonary system. Peripheral blood (PB) specimens were procured from patients devoid of any prior treatment history. Patients were enrolled in the Department of Hematooncology and Bone Marrow Transplantation of the Medical University of Lublin (Lublin, Poland). The median follow-up time was 48 months, ranging from 1 to 72. The clinical staging was ascertained utilizing the Rai classification system [31]. Additionally, the investigation incorporated an examination of various clinical and biological parameters, including white blood cell (WBC) count, lymphocyte count, levels of lactate dehydrogenase (LDH) and β2-microglobulin (β2M), CD38 expression (defined as positive if expressed by $\geq$30% of CLL cells), zeta-chain-associated protein kinase 70 (ZAP-70) expression (cut-off 20%), and cytogenetic abnormalities. The baseline characteristics observed in this cohort are comprehensively summarized in Table 1. Control PB samples were derived from 40 healthy volunteers (HVs). The control group, with an age range of 35–64 years and a median of 55 years, comprised 13 females and 27 males. For the HV group, the following criteria had to be met: lack of cancer, autoimmune, pulmonary, and cardiovascular diseases. The study protocol was approved by the Ethics Committee of the Medical University of Lublin. Written informed consent was obtained from all donors. Patients were recruited from January 2016 to January 2023.

Gal-9 Detection in Plasma

Plasma anticoagulated with ethylenediaminetetraacetic acid (EDTA) was employed in the test. Human Galectin-9 ELISA Kit (Cat. No. EH206RB; Thermo Fisher Scientific, Waltham, MA, USA) was used to detect plasma Gal-9 levels in accordance with the manufacturer's instructions. The measurement was conducted in duplicate. Viktor3 and Workout 2.0 software (Perkin Elmer, Waltham, MA, USA) were used to determine the optical density at a wavelength of 450 nm. The detection limit for Gal-9 was 36 pg/mL.

Peripheral Blood Mononuclear Cells (PBMCs) Isolation

The collection of PB samples was done in tubes containing EDTA and processed immediately. PBMCs were isolated by density gradient centrifugation using Lymphocyte Separation Medium 1077 (Cat No. C-44010, PromoCell, Heidelberg, Germany). Samples were centrifuged at 700 ×g for 20 minutes at room temperature (RT). Interphase cells were collected and washed twice in phosphate-buffered saline (PBS).

Identifying B Cells With Gal-9 Expression

PBMCs were stained with the phycoerythrin (PE) anti-Galectin-9 (Clone 9M1-3; Cat No. 565890; BD Biosciences Franklin, Lakes, NJ, USA) and fluorescein isothiocyanate (FITC) anti-CD19 (Clone HIB19; Cat No. 555412; BD Biosciences) monoclonal antibodies (MoAbs). Cells were incubated for 20 minutes at room temperature. A concentration of about 1×10^6 cells/mL was used for analysis. Data acquisition was performed on a Cytoflex LX with CytExpert software (Beckman Coulter, Brea, CA, USA). The analysis of the data was done with Kaluza software, 2.1.1 version (Beckman Coulter, Brea, CA, USA). The gating was set using fluorescent minus one (FMO) controls.

Gal-9 Expression on the B Cell Membrane Visualized by Confocal Microscopy

Confocal microscopy was used to visualize the localization of Gal-9 on the B cell membrane. We noticed that many antibodies may be used in both flow cytometry and fluorescence microscopy. This was the reason why in some experiments, we took a portion of cells stained for flow cytometry analysis (as described above). Samples were subsequently fixed with 4% paraformaldehyde, permeabilized with 70% ethanol, and washed 3 times in PBS. Cells were then sedimented onto glass microscope slides by cytocentrifugation. After mounting on microscope slides, nuclei were counterstained with 1 µg/mL of 4′,6-diamidino-2-phenylindole (DAPI) (Thermo Fisher Scientific, Waltham, MA, USA; Cat No. D1306) for 15 minutes at room temperature. A Nikon A1R confocal microscope (Nikon, Tokyo, Japan) was used to perform imaging. A 488 nm argon laser was used to excite FITC fluorescence, and a 525 nm spectral filter was used to measure it. 561 and 405 nm lasers and 595 and 450 nm filters were applied for PE and DAPI, respectively.

Identifying $CD19^+CD5^+CD24^{hi}CD38^{hi}$ B Regulatory Cells (Breg) Among $CD19^+$ Cells

The next step was to use flow cytometry to detect the Gal-9^+ expression among $CD19^+CD5^+CD24^{hi}CD38^{hi}$ Breg in 11 CLL patients. All MoAbs were from BD Biosciences (Franklin, Lakes, NJ, USA): FITC anti-CD19 (Clone HIB19; Cat No. 555412), V450 anti-CD5 (Clone UCHT2; Cat No. 561154); PE anti-Galectin-9 (Clone 9M1-3; Cat No. 565890), allophycocyanin (APC) anti-CD38 (Clone HIT2; Cat No. 555462), and PE-Cy7 anti-CD24 (Clone ML5; Cat No. 561646). The PBMCs were stained for 20 minutes and then washed in PBS before being acquired using Cytoflex LX with CytExpert software (Beckman Coulter, Brea, CA, USA). Flow cytometry analysis of the $CD19^+CD5^+CD24^{high}CD38^{high}$ cells was performed among $CD19^+CD5^+$ B cells. Moreover, the percentage of Gal-9 positive cells within the $CD19^+CD5^+CD24^{high}CD38^{high}$ Breg and non-Breg CLL cells ($CD19^+CD5^-CD24^+CD38^{low}$) was examined.

Identifying MDSC Subpopulations With Gal-9 Expression

The percentage of three major MDSC subpopulations was assessed: M-MDSC ($CD14^+$human leukocyte antigen (HLA)-$DR^{low/-}CD15^-$), PMN-MDSC ($CD11b^+CD14^-CD15^+$), and eMDSC (Lin^-HLA-$DR^{low/-}CD11b^+CD33^+$). Furthermore, Gal-9 expression was evaluated in those MDSC subsets. The expression of Gal-9 on MDSC subsets was analyzed in 40 patients. PBMCs were stained with the following anti-human monoclonal antibodies: PE/Cyanine7 anti-HLA-DR; (Clone L243; Cat No. 307616; BioLegend, San Diego, CA, USA), APC anti-Lineage Cocktail (CD3, CD14, CD16, CD19, CD20, CD56; Clone: UCHT1; HCD14; 3G8; HIB19; 2H7; HCD56; Cat No. 348803; BioLegend, San Diego, CA, USA), V450 anti-CD11b (Clone ICRF44; Cat No. 560480; BD Biosciences, Franklin, Lakes, NJ, USA), FITC anti-CD14 (Clone M5E2; Cat No. 555397; BD Biosciences, Franklin, Lakes, NJ, USA), APC anti-CD15 (Clone HI98; Cat No. 551376; BD Biosciences, Franklin, Lakes, NJ, USA), FITC anti-CD33 (Clone HIM3-4; Cat No. 555626; BD Biosciences, Franklin, Lakes, NJ, USA), and PE anti-Galectin-9 (Clone 9M1-3; Cat No. 565890; BD Biosciences, Franklin, Lakes, NJ, USA). The samples were stained for 20 minutes at room temperature and washed with PBS before being acquired with the Cytoflex LX with CytExpert software (Beckman Coulter, Brea, CA, USA). MDSC subpopulation phenotypes were established as suggested by Bronte *et al.* [32].

The Isolation of $CD19^+$ Cells

The separation of B cells from PBMCs was done through the use of CD19 Microbeads (Cat No. 130-050-301, Miltenyi Biotec, Bergisch Gladbach, Germany). The manufacturer's procedure was followed. The cells that were obtained were found to be over 95% pure, as determined by flow cytometry.

Digital PCR (dPCR)

The total RNA was extracted from purified B lymphocytes using the QIAamp RNA Blood Mini Kit (Cat No. 52304, Qiagen GmbH, Hilden, Germany), in accordance with manufacturer's protocol. A BioSpec nano-

spectrophotometer (Shimadzu, Kyoto, Japan) was utilized to evaluate RNA quality and quantity, and a reverse transcription (RT) reaction was conducted with 10 ng of total RNA. Generation of complementary DNA (cDNA) was done by using the QuantiTect Reverse Transcription kit (Cat No. 205311, Qiagen GmbH, Hilden, German). The concentration of *Gal-9* transcripts was measured using dPCR. Duplexed analysis was performed on samples for Gal-9 (6-carboxyfluorescein (FAM)-labeled; assay ID: Hs00247135_m1, Thermo Fisher Scientific, Waltham, MA, USA) and endogenous control Glyceraldehyde-3-phosphate dehydrogenase (GAPDH) (proprietary fluorescent dye (VIC)-labeled; Cat No. 4310884E, Thermo Fisher Scientific, Waltham, MA, USA) using the QIAcuity Probe PCR Kit (Cat No. 250101, Qiagen GmbH, Hilden, Germany), master mix for microfluidic use in the QIAcuity Nanoplates. 8.5K 24-well Nanoplates (Cat No. 250011, Qiagen GmbH, Hilden, Germany) were used to perform PCR reactions as per the manufacturer's protocol. The conditions for thermocycling were as follows: 2 minutes at 95 °C followed by 40 cycles of 15 seconds at 95 °C and 1 minute at 60 °C. Digital PCR instrument (QIAcuity One) and QIAcuity Software Suite v.2.5.0.1 from Qiagen GmbH (Hilden, Germany) were used. Copy Number Variation (CNV) with reference target was used in QIAcuity Software to estimate copy numbers. The CNV is given by the ratio of absolute concentrations of target and reference genes (*GAPDH*) within a sample. Digital PCR was performed in a subset of randomly selected 36 CLL patients to ensure an unbiased representation of the whole population.

Epstein–Barr Virus DNA Quantitative Assay

The methods previously reported were used for the detection of EBV DNA in purified $CD19^+$ cells [23]. The detection of EBV DNA was accomplished using the EBV PCR Kit (Cat No. EBV/ISEX/100; GeneProof, Brno, Czech Republic). The target sequence (*EBNA-1*; EBV nuclear antigen 1 gene) was amplified using a 7300 Real-Time PCR System (Applied Biosystems, Inc., Waltham, MA, USA). The standard curve was utilized to quantify EBV DNA. EBV PCR kit allows linear quantification of 10^1 to 10^4 EBV DNA copies (cp) per µL. Subsequently, the viral load concentration in cp/mL was calculated according to the manufacturer's instructions.

EBV-miR-BHRF1-1 Detection

Total RNA from 86 CLL patients was isolated from purified $CD19^+$ cells using the mirVana miRNA Isolation Kit (Cat No. AM1560, Thermo Fisher Scientific, Waltham, MA, USA). RNA (10 ng) was reverse transcribed to complementary DNA (cDNA) using TaqMan MicroRNA Reverse Transcription Kit (Cat No. 4366596, Thermo Fisher Scientific, Waltham, MA, USA). cDNA samples were used for EBV-miR-BHRF1-1 expression analysis, carried out with TaqMan Universal PCR Master Mix II (Cat No. 4440043, Thermo Fisher Scientific, Waltham, MA, USA) and ready-to-use, commercially available TaqMan assays from Thermo Fisher Scientific (Waltham, MA, USA): ebv-miR-bhrf1-1 (Assay ID 007757). Reverse transcription quantitative polymerase chain reaction (RT-qPCR) reactions were performed using the Applied Biosystems 7300 Real-Time PCR System (Applied Biosystems, Inc., Waltham, MA, USA). The level of the EBV-miR-BHRF1-1 expression was normalized to RNU6B (Assay ID: 001093, Thermo Fisher Scientific, Waltham, MA, USA) as endogenous control, and the relative expression of miRNA was calculated using the $2^{-\Delta\Delta Ct}$ formula. The cycle conditions for EBV-miR and RNU6B were one cycle for 10 minutes at 95 °C, then 40 cycles (15 seconds at 95 °C, and 60 seconds at 60 °C).

Examining the Expression of CD38 and ZAP-70

Using previously published methods, ZAP-70 and CD38 were detected in $CD19^+/CD5^+$ cells [33,34]. Leukemic B-cells were identified using MoAbs anti-CD19 FITC (clone SJ25C1, Cat No. 340409) and anti-CD5 PE-Cy5 (clone UCHT2, Cat No. 555354). The use of anti-CD38 PE (clone HIT2, Cat No. 555460) or anti-ZAP-70 PE (clone 1E7.2, Cat No. 344636) enabled the detection of $CD19^+CD5^+$ cells that expressed CD38 or ZAP-70. All MoAbs were obtained from BD Biosciences (Franklin, Lakes, NJ, USA). Antibodies that target surface markers were incubated with cells for 20 minutes at room temperature. Afterward, for intracellular ZAP-70 staining, samples were fixed/permeabilized using the Cytofix/Cytoperm Fixation/Permeabilization Kit (Cat No.554714, BD Biosciences, Franklin, Lakes, NJ, USA). BD Biosciences' FACSCalibur instrument with CellQuest Pro Software (BD Biosciences, Franklin, Lakes, NJ, USA) was utilized. The cut-off point for ZAP-70 expression was $\geq$20%, while for CD38 expression, it was $\geq$30%.

Interphase Fluorescence In Situ Hybridization (I-FISH Analysis)

Fluorescence in situ hybridization (FISH) method was used to analyse cytogenetic abnormalities in leukemic cells. The analysis was based on commercially available FISH probes (Abbott GmbH, Wiesbaden, Germany): Vysis CLL FISH Probe Kit (Cat. No. 04N02-22). Mononuclear cells were cultured in Roswell Park Memorial Institute (RPMI) 1640 medium for 24 hours without mitogen stimulation. Cell suspensions were placed on microscopic slides and utilized for FISH after being hypotonic and methanol-acetic acid 3:1 fixed. For each probe, at least 200 nuclei were examined. The threshold for positive results was 2.5% (mean $\pm$ standard deviation (SD)). An OLYMPUS BX51 fluorescence microscope (Olympus, Tokyo, Japan) was used in the analysis. The FISH protocol was described previously [35].

Statistical Analysis

Data was analyzed in Statistica 13.3 software (StatSoft, Cracow, Poland) and GraphPad Prism 9 (GraphPad Software, San Diego, CA, USA). The Shapiro-Wilk test was utilized to assess the data distribution. For group comparisons, the U Mann-Whitney or Kruskal-Wallis with Dunn correction tests were performed for two-group or multiple-group comparisons, respectively. The data is displayed as the median with the interquartile range (IQR). The degree of association between variables was measured using Spearman's rank correlation. The time period from the diagnosis to the beginning of the first treatment, or the date of death or last follow-up, during which the patient was known to be untreated, was defined as time to first treatment (TTFT). The overall survival (OS) was defined as the period from the date of diagnosis to the date of death or last follow-up. Survival analyses were performed using Kaplan-Meier methodology and the log-rank test. Univariate Cox regression analysis was used for the initial screening of prognostic variables. The independent risk factors that affect the prognosis of CLL patients were identified through multivariate Cox regression analysis. The optimal cut-point value was chosen based on the receiver operating characteristics (ROC) analysis. ROC curve analysis was conducted using the Youden Index. The sensitivity, specificity, and area under the curve (AUC) were provided. $p < 0.05$ was seen as statistically significant.

Results

The Galectin-9 Plasma Levels

Levels of Gal-9 in plasma obtained from healthy controls were significantly lower ($p = 0.006$) than those from CLL subjects (Fig. 1A). The association between baseline variables (Table 1) and the concentration of Gal-9 in CLL patients was examined. Spearman's correlation analysis did not reveal a statistically significant correlation between Gal-9 plasma level and leukocytosis ($\rho = 0.012$, $p = 0.897$), lymphocytosis ($\rho = 0.010$, $p = 0.811$), or β2-microglobulin level ($\rho = 0.027$, $p = 0.624$). There was no association between Gal-9 concentration and the age ($\rho = 0.223$, $p = 0.145$) and gender of the patients studied ($p = 0.848$). The concentration of Gal-9 has been found to significantly increased ($p = 0.001$) in patients at high risk (stage III/IV) of CLL progression compared to stage 0 (Fig. 1B). A significantly higher plasma level of Gal-9 was observed in ZAP-70-positive and CD38-positive groups compared to ZAP-70-negative ($p = 0.03$, Fig. 1C) and CD38-negative ($p = 0.04$, Fig. 1D) ones. However, there were no differences in Gal-9 levels ($p = 0.77$) when patients were divided based on immunoglobulin heavy-chain variable region (*IGHV*) mutational status (Fig. 1E). Patients with 11q22.3 deletion, 17p13.1 deletion and/or trisomy 12 had a higher concentration of Gal-9 than those without these unfavorable cytogenetic abnormalities ($p = 0.02$, Fig. 1F).

The Membrane Expression of Gal-9 on B CD19$^+$ Cells

Our previous research indicated that *Gal-9* mRNA expression was upregulated in malignant B cells from patients with CLL. RT-qPCR was used to quantify *Gal-9* mRNA expression in CLL cells [23]. The current study used digital PCR to confirm these results. Similarly, in the current study, the *Gal-9* mRNA levels were significantly higher ($p < 0.0001$) in B cells from CLL patients compared to healthy volunteers (Fig. 2).

Our goal was also to confirm these results by examining Gal-9 membrane expression. CD19$^+$ B cells with Gal-9 expression were identified through flow cytometry analysis. The gating strategy to identify Gal-9-positive B cells is shown in Fig. 3. The combination of forward scatter area (FSC-A) and forward scatter height (FSC-H) allowed for the exclusion of doublets. Subsequently, mononuclear cells were identified from the singlets based on side scatter area (SSC-A) and FSC-A properties. Then, selected PBMCs were analyzed for CD19$^+$ expression (SSC-A vs CD19 FITC). The use of FMO control enabled the definition of a boundary gate between positive and negative Gal-9 expression. The analysis of B cells with Gal-9 expression was done within gated CD19$^+$ lymphocytes (Fig. 3).

Confocal microscopy was employed to demonstrate Gal-9's localization on the membrane of B cells (Fig. 4A,B). Fig. 4 shows a view of a cluster of anti-Gal-9 antibody binding cells (red fluorescence), all of which also bind anti-CD19 (green fluorescence), a B cell marker. A red and green ring of fluorescence was found (Fig. 4A,B), which suggests that it is located in the membrane. To analyze the colocalization of the tested molecules, the resulting images were superimposed. As a result, in addition to signals in colors corresponding to the fluorochromes used (PE and FITC), in the places of co-occurrence of the studied molecules, an intermediate color is visible between the colors of fluorescence of colocalizing antigens.

In the control group, the median percentage of Gal-9-positive B cells was significantly lower than that of CLL patients ($p = 0.04$) (Fig. 5A). Healthy controls had low variability in the percentage of CD19$^+$/Gal-9$^+$ cells. In contrast, patients with CLL exhibited significantly varied values. The median percentage of Gal-9-positive B cells in Stage 0 patients was significantly lower than in stages III-IV according to Rai stages ($p = 0.004$, Fig. 5B). The percentage of CD19$^+$/Gal-9$^+$ cells was significantly higher in ZAP-70-positive patients compared to ZAP-70-negative ones ($p = 0.01$, Fig. 5C). We observed a significantly lower percentage of CD19$^+$ cells with Gal-9 expression in CD38-negative patients compared to CD38-positive ones ($p = 0.01$) (Fig. 5D). There was no statistical association between Gal-9 expression and *IGHV* mutation status ($p = 0.32$, Fig. 5E). On the other hand, within the cohort of patients harboring del(11q22), del(17p13), and/or trisomy 12 aberrations, Gal-9 expression was significantly higher ($p =$

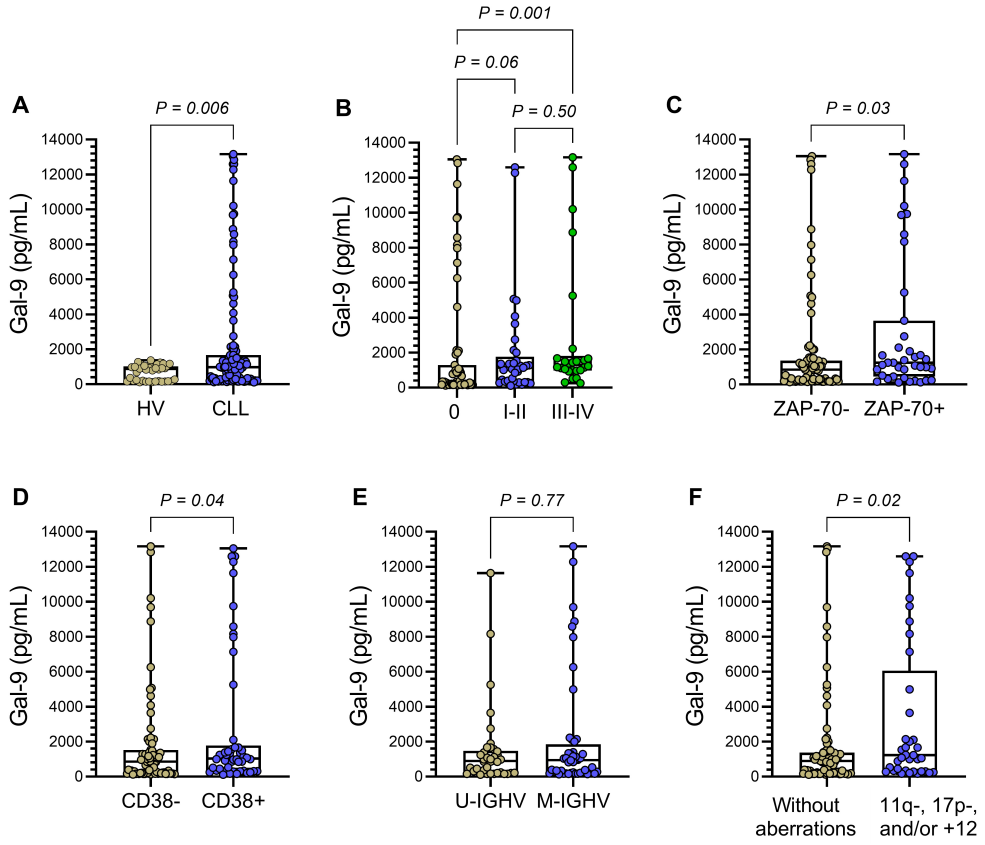

Fig. 1. Plasma concentrations of Gal-9. (A) Comparison of Gal-9 plasma level between CLL patients and healthy volunteers (HVs). (B–F) Patients were stratified based on Rai stage (B), ZAP-70 status (C), CD38 expression (D), *IGHV* mutation status (E), and chromosomal abnormalities (F). *p*-values were calculated using the Mann-Whitney U test (for two-group comparisons) or the Kruskal-Wallis test with Dunn's post hoc correction (for multiple groups). *IGHV*, immunoglobulin heavy-chain variable gene; U-IGHV, unmutated IGHV; M-IGHV, mutated IGHV; Gal-9, Galectin-9; CLL, chronic lymphocytic leukemia; ZAP-70, zeta-chain-associated protein kinase 70.

0.008) compared to the group lacking these genetic abnormalities (Fig. 5F).

Gal-9 Plasma Levels Were Correlated With Gal-9-Positive MDSCs and B-Cells

We confirmed our previous findings [24] that M-MDSC are significantly increased in CLL patients compared to healthy volunteers [median (IQR), 12.810 (2.340–30.850)% vs 3.210 (0.410–5.770)%, $p < 0.001$] (Fig. 6A). Additionally, in the CLL patients, PMN-MDSC subpopulation was significantly higher than in healthy controls [median (IQR), 5.047 (0.060–9.339)% vs 1.050 (0.200–7.900)%, $p < 0.001$] (Fig. 6B). eMDSC did not differ significantly [median (IQR), 1.350 (0.010–6.710)% vs 0.325 (0.004–3.500)%, $p = 0.08$] (Fig. 6C). The percentages of M-MDSC/Gal-9$^+$ and eMDSC/Gal-9$^+$ were significantly higher than the percentage of PMN-MDSC subpopulation with Gal-9 expression ($p < 0.001$ and $p = 0.002$, respectively) (Fig. 6D). The gating strategy for identifying MDSC subsets with Gal-9 expression was shown in Fig. 7.

Then we paired the percentage of Gal-9-positive MDSC with the Gal-9 plasma level (Fig. 8A–C). We found that Gal-9 levels positively correlated with the percentage of eMDSC/Gal-9$^+$ ($\rho = 0.562$, $p < 0.001$) (Fig. 8A). Similarly, there was a significant positive correlation of the Gal-9$^+$ M-MDSC with the plasma level of Gal-9 ($\rho = 0.518$, $p = 0.001$, Fig. 8B). However, the percentage of PMN-MDSC/Gal-9$^+$ did not correlate to the Gal-9 plasma level ($\rho = 0.323$, $p = 0.08$, Fig. 8C). The study revealed that Gal-9 plasma concentration was associated with the Gal-9 expression level in the malignant B cells ($\rho = 0.596$; $p < 0.001$, Fig. 8D).

Association of Gal-9 Expression on B Cells With EBV Status

Our previous study indicated that EBV-positive CLL patients had a significantly higher level of *Gal-9* mRNA than EBV-negative ones [23]. In the present study, we observed that the plasma concentration of Gal-9 ($p = 0.03$, Fig. 9A) and the percentage of B cells with Gal-9 expression ($p = 0.02$, Fig. 9B) were significantly higher in EBV-positive CLL cases.

Table 1. The characteristics of CLL patients at the initial assessment.

Characteristics	CLL patients (n = 126)	Healthy volunteers (n = 40)
Gender		
Female	60	13
Male	66	27
Age (years)		
Median (IQR)	66 (60–72)	55 (50–60)
Min–max	45–80	35–64
Rai Stage		
Rai Stage 0 (low risk)	63	
Rai Stages I–II (Intermediate risk)	37	
Rai Stages III–IV (High risk)	26	
ZAP-70 (cut-off 20%)		
ZAP-70 $\geq$20%	39	
ZAP-70 $<$20%	87	
CD38 (cut-off 30%)		
CD38 $\geq$30%	50	
CD38 $<$30%*	76	
Genetic abnormalities (FISH)		
17p-	16	
11q-	14	
+12	6	
Without 17p-, 11q-, +12	90	
IGHV mutational status		
Mutated	48	
Unmutated	39	
Unavailable	39	
EBV status		
Positive	30	
Negative	48	
Unavailable	48	
Patients receiving treatment throughout the observation period	58	
Type of treatment		
Fludarabine, cyclophosphamide, and rituximab	19/58	
Bendamustine and rituximab	12/58	
Chlorambucil and obinutuzumab	16/58	
Venetoclax and obinutuzumab	8/58	
Acalabrutinib	2/58	
Ibrutinib	1/58	
Patients' initial laboratory data		
WBC (G/L), median (IQR)	24.63 (17.2–55.16)	
Lymphocyte count (G/L), median (IQR)	18.32 (10.87–47.58)	
LDH level (IU/L), median (IQR)	349 (285–412)	
β2M level (mg/dL), median (IQR)	2.60 (2.08–3.40)	

EBV, Epstein-Barr virus; WBC, white blood cell; LDH, lactate dehydrogenase; β2M, β2-microglobulin; IQR, interquartile range; *IGHV*, immunoglobulin heavy-chain variable gene; ZAP-70, zeta-chain-associated protein kinase 70; CLL, chronic lymphocytic leukemia; FISH, fluorescence in situ hybridization.

The Expression of Gal-9 Was Correlated With the Expression of EBV-miR-BHRF1-1

The investigation was carried out to examine whether EBV-miRBHRF1-1 expression in CLL cells was correlated with B cell percentage with Gal-9 expression. The percentage of $CD19^{+}$/Gal-9^{+} significantly correlated with the expression of EBV-miR-BHRF1-1 (ρ = 0.628, p = 0.016, Fig. 10A). Furthermore, we analyzed the EBV-miR-BHRF1-1 expression in CLL cells by splitting our cohort based on the cut-off for $CD19^{+}$/Gal-9^{+} percentage ($>$28.03). We found a significant increase of EBV-miR-BHRF1-1 in the CD19/Gal-9^{high} group compared to

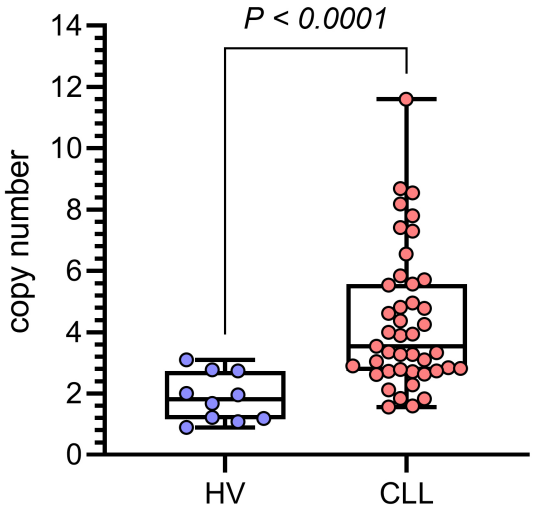

Fig. 2. Transcript levels of *Gal-9* gene (LGALS9) measured by digital PCR (dPCR). *Gal-9* transcript copy number determined in B cells from 36 CLL patients and 10 healthy volunteers (HVs). *P-values* were calculated using the Mann-Whitney U test. CLL, chronic lymphocytic leukemia.

CD19/Gal-9^{low} group [median (IQR), 6.58 (1.10–25.98) vs. 0.52 (0.18–2.47), $p = 0.0011$, Fig. 10B]. In addition, in 30 subjects with a positive EBV-DNA test, there was a significant, but weak association between the EBV-DNA copy number and the percentage of B cells with Gal-9 expression ($\rho = 0.427$, $p < 0.001$, Fig. 10C).

The Breg Phenotype Is Observed in B Cells that Express Gal-9

Considering that EBV latency III transformed B cells display an immunosuppressive profile similar to Breg [36], we analyzed the association of Gal-9$^+$ B cells with the B regulatory cells (Fig. 11A–D). We noted that a subset of leukemic B cells phenotypically resembles transitional Breg (CD19$^+$CD5$^+$CD24^{high}CD38^{high}) (Fig. 11B). We observed that Gal-9 expression was significantly higher ($p < 0.0001$) within the CD19$^+$CD5$^+$CD24^{high}CD38^{high} fraction of CLL cells (Breg) relative to the CD19$^+$CD5$^+$CD24$^+$CD38^{low} fraction (non-Breg CLL cells) (Fig. 11E).

The Clinical Findings and Gal-9 Expression in CLL Patients

Fifty-eight patients required treatment during the observation period (Table 1). The concentration of Gal-9 in the plasma of treated patients was significantly higher ($p = 0.003$) than those without treatment (Fig. 12A). Similarly, the percentage of CD19$^+$/Gal-9$^+$ cells measured when it's diagnosed was higher for patients who required therapy than for those who did not require treatment during the observation period ($p = 0.02$, Fig. 12B).

Our research focused on Gal-9's potential role as a prognostic factor in CLL by splitting our cohort into two groups based on the plasma level of Gal-9 or the percentage of cells positive for Gal-9. The cut-off value for plasma Gal-9 concentration was established utilizing the ROC analysis and was >1535.51 (AUC, 0.762; 95% confidence interval [CI], 0.659–0.866; $p < 0.0001$; Fig. 13A). The cut-off for the percentage of Gal-9-positive B cells was >28.03 (AUC, 0.711; 95% CI, 0.569–0.854; $p = 0.004$; Fig. 13B). According to our study, Gal-9 concentrations exceeding 1535.51 pg/mL significantly ($p = 0.006$) impacted the time to first treatment (TTFT) (Fig. 13C, Table 2). In the same way, Gal-9-positive B cells that were over 28.03% were found to be significantly ($p = 0.004$) associated with a shorter TTFT (Fig. 13D, Table 2). In addition, univariate and multivariate Cox regression analysis showed that the percentage of Gal-9 positive B cells was an independent prognostic factor for TTFT in CLL patients ($p = 0.006$) (Table 2).

Then, in a similar manner, we tested if serum Gal-9 and Gal-9$^+$ B cells have any impact on the overall survival of CLL patients. In univariate analysis, the Gal-9 plasma concentration (hazard ratio [HR] 0.265; 95% CI 0.076–0.921; $p = 0.656$) and percentage of B cells with Gal-9 expression (hazard ratio [HR] 0.969; 95% CI 0.342–2.738; $p = 0.952$) did not appear to have a significant impact on overall survival.

Discussion

CLL development is heavily influenced by interactions between leukemic cells and various components of the tumor microenvironment (TME) [37]. Dysregulation of immune compensatory mechanisms in CLL leads to clonal proliferation, migration, and resistance to treatment. Evidence suggests a crucial role of immune checkpoints in CLL pathogenesis [38]. Gal-9, a key immune checkpoint ligand, remains incompletely understood in its role in CLL pathogenesis [21]. Our previous research indicated that *Gal-9* mRNA expression (quantified with RT-qPCR) was upregulated in leukemic B cells from patients with CLL. The expression of *Gal-9* mRNA was strongly correlated with negative prognostic markers. We suggested Gal-9 as a novel biomarker for CLL [23]. Digital PCR was utilized in this study to verify the upregulation of *Gal-9* mRNA in leukemic cells. Our goal was also to confirm these results, given Gal-9 expression at the protein level, this time in a larger group of CLL patients. We evaluated the expression of Gal-9 using multicolor flow cytometry and ELISA methods. Wdowiak *et al.* [21], Pang *et al.* [39], and Alimu *et al.* [22] conducted studies that revealed an elevated serum Gal-9 level in patients with CLL. This is consistent with our findings. Our data is also in line with those reported by Taghiloo *et al.* [40] who observed a significant increase in Gal-9 expression in PBMCs derived from CLL compared

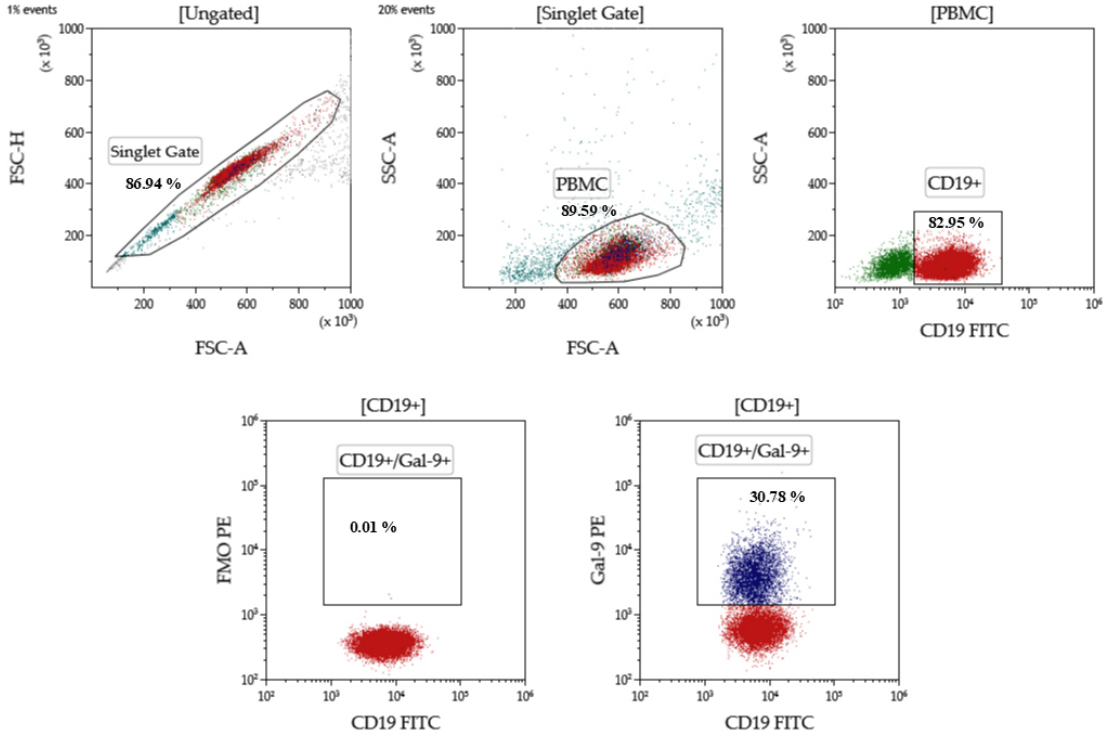

Fig. 3. The gating strategy for the identification of Gal-9-positive B cells. Each dot plot's title displays the input gate. Kaluza 2.1.1 software (Beckman Coulter, Brea, CA, USA) was employed for data analysis. B cells with Gal-9 expression were analyzed within gated $CD19^{+}$ lymphocytes. The gating was set using fluorescent minus one (FMO) controls. FITC, fluorescein isothio- cyanate; PE, phycoerythrin; FSC-H, forward scatter height; SSC-A, side scatter area; PBMC, peripheral blood mononuclear cells; Gal-9, Galectin-9.

Table 2. Univariate and multivariate analysis of TTFT.

Risk Factors	Univariate analysis			Multivariate analysis		
	HR	95% CI	*p*-value	HR	95% CI	*p*-value
ZAP-70 expression >20%	1.778	1.204–2.626	0.003	1.483	0.949–2.315	0.083
CD38 expression >30%	1.443	0.967–2.152	0.072		NA	
β2M level >3.5 mg/dL	3.331	2.217–5.006	<0.0001	3.248	2.138–4.937	<0.0001
Positive 17p- and/or 11q-	2.036	1.323–3.135	0.001	1.672	1.111–2.512	0.013
Age >65 years	1.302	0.872–1.941	0.196		NA	
Gal-9-positive B cells >28.03%	2.585	1.333–5.003	0.004	2.722	1.339–5.535	0.006
Gal-9 plasma level >1535.51 pg/mL	2.116	1.236–3.626	0.006	1.631	0.956–0.781	0.072

Variables with $p < 0.05$ in the univariate analysis were used for the multivariate analysis. HR, hazard ratio; 95% CI, 95% confidence interval; NA, not assessed. Time to first treatment (TTFT) was defined as the number of months between the date of diagnosis and the date of initial therapy.

to healthy controls. Notably, we verified their findings in a larger cohort of 126 patients diagnosed with CLL. In our study, elevated plasma Gal-9 levels and higher percentages of Gal-9 positive B-cells correlated with the clinical stage of CLL according to the Rai classification. This agrees with Alimu *et al.* [22] and Wdowiak *et al.* [21] who observed that the level of Gal-9 in CLL is significantly different among the three Binet stage groups. The Rai and Binet staging systems are still the backbone of prognostication in clinical practice. These traditional clinical staging systems support the decision for treatment initiation, but neither can accurately predict early disease progression [41,42]. A plethora of different prognostic factors in CLL have been discovered over recent decades [43,44]. Markers, such as cytogenetic abnormalities, mutation status of IGHV, CD38, and ZAP-70, have enabled the subdivision of CLL patient populations into risk groups with favorable and unfavorable prognosis [41,42]. In the currently conducted research, higher concentrations of Gal-9 and the percentage of B cells that show Gal-9 expression were observed in ZAP-70-positive and CD38-positive patients. Our previous study found that malignant B-cells from CLL patients with unmutated *IGHV* had a significantly higher relative expression of *Gal-9* mRNA [23]. Sadly, we haven't veri-

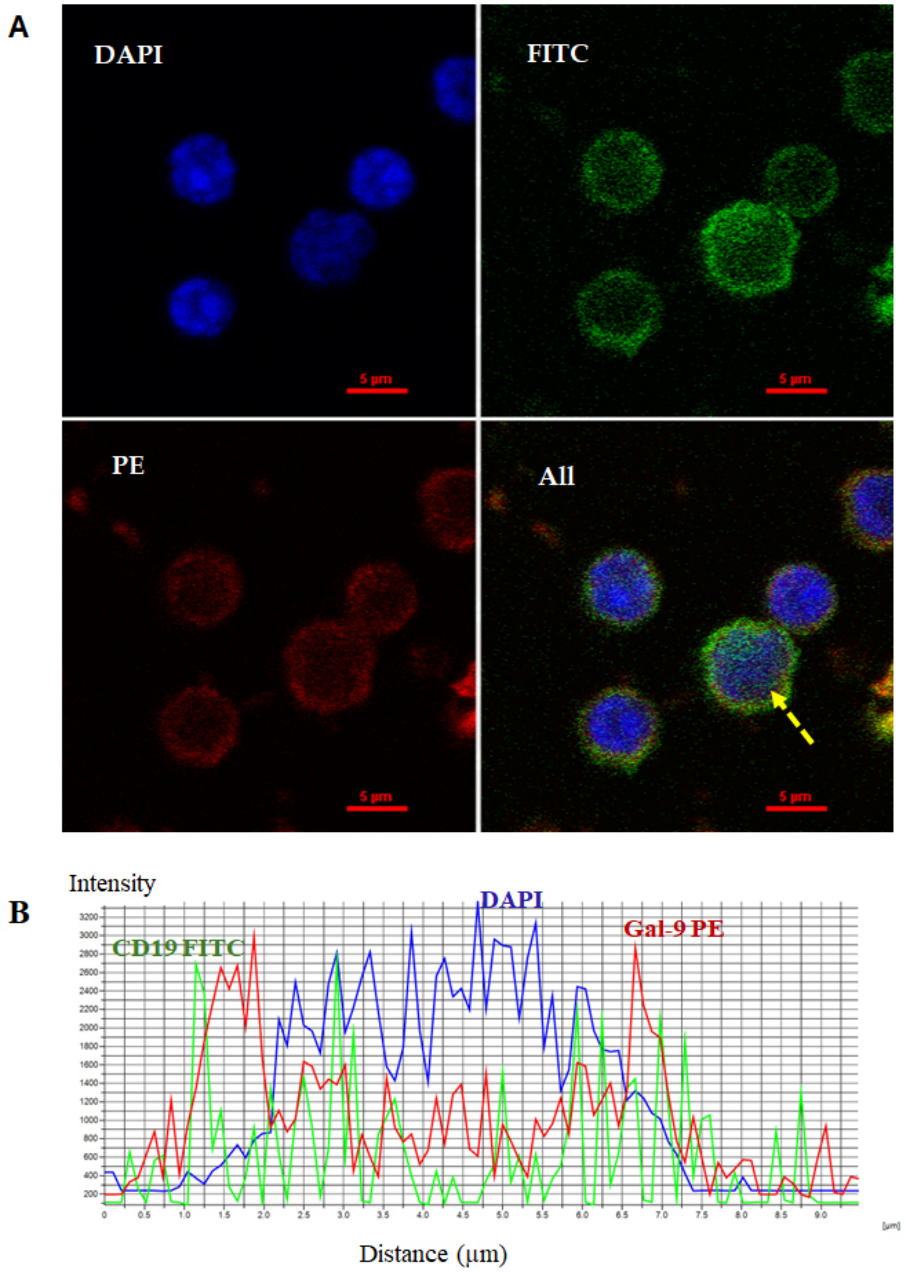

Fig. 4. Detection of Gal-9 expression in CD19$^+$ cells via confocal microscopic imaging. (A) The representative cells' images were shown in individual and merged fluorescent channels that overlayed DAPI, FITC, and PE fluorescence. The membrane staining of CD19 (FITC) is green, while the membrane staining of Gal-9 (PE) is red. The nucleus was stained with DAPI. Its blue fluorescence vividly contrasts with the red and green fluorescent dyes used to stain Gal-9 and CD19, respectively. (B) The fluorescence intensity profile of DAPI, CD19, and Gal-9 from one representative cell (marked with a yellow arrow in panel A). A Nikon A1R confocal microscope (Tokyo, Japan) was used to perform imaging. DAPI, 4′,6-diamidino-2-phenylindole; FITC, fluorescein isothiocyanate; PE, phycoerythrin; Gal-9, Galectin-9.

fied this in our current studies by evaluating Gal-9 expression at the protein level. It's possible that the absence of *IGHV* status for all patients was the cause. It is worth pointing out that likewise, the connection between CD38 expression and *IGHV* mutation status is not unambiguous, and CD38 expression may change over the course of the disease [45]. Nevertheless, there was a statistically significant connection of Gal-9 expression with other poor prognostic features, i.e., the presence of 11q22.3 deletion, 17p13.1 deletion, and/or trisomy 12. This is in accordance with Wdowiak and co-authors' study [21] that showed higher Gal-9 serum levels in CLL patients with 11q and 17p deletions. It should be remembered that deletions of 11q, 17p, and trisomy 12 are well-known prognostic factors and are

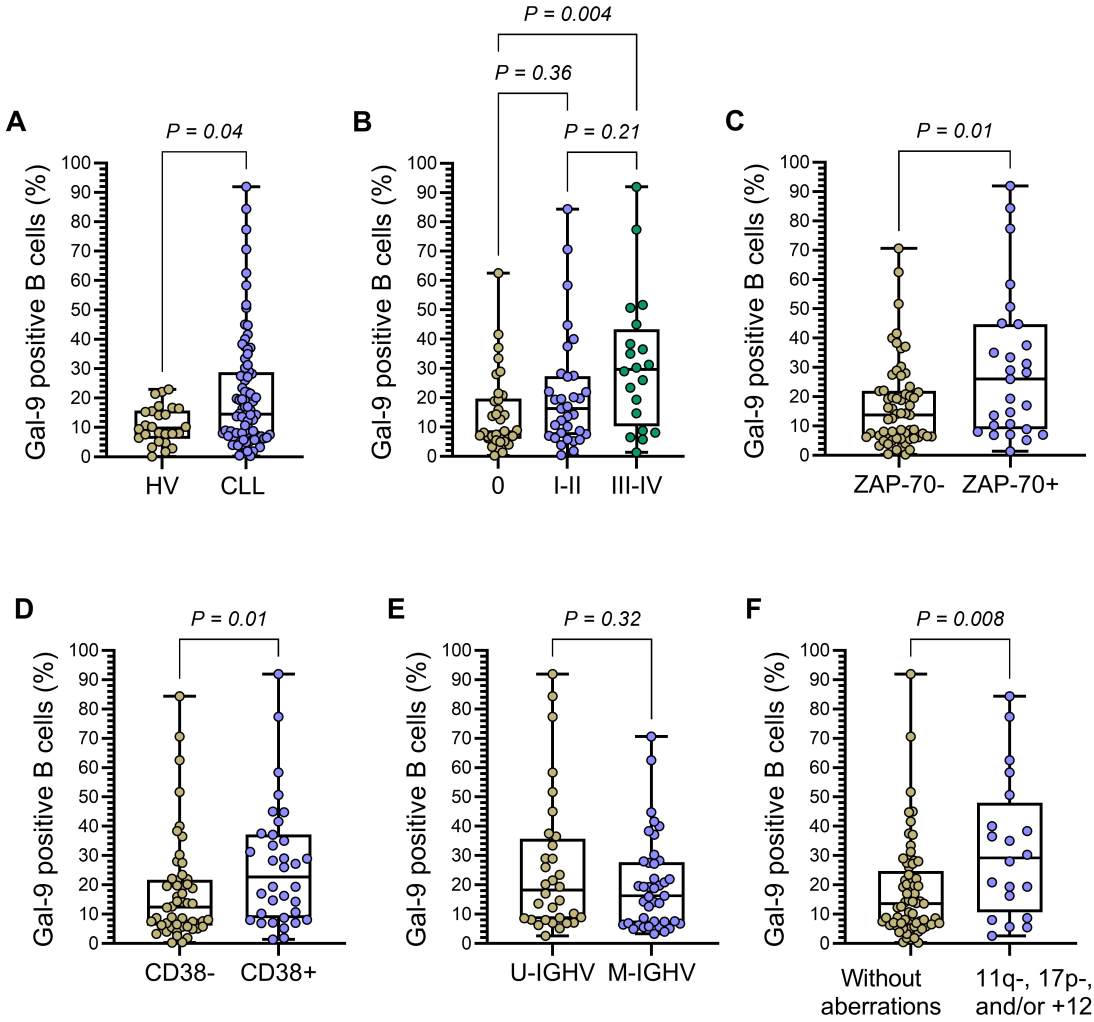

Fig. 5. Percentage of Gal-9 positive B-cells. (A) Comparison of $CD19^+$ B cells expressing Gal-9 between CLL patients and healthy volunteers (HVs). (B–F) Patients were stratified based on Rai stage (B), ZAP-70 status (C), CD38 expression (D), *IGHV* mutation status (E), and chromosomal abnormalities (F). *p*-values were calculated using the Mann-Whitney U test (for two-group comparisons) or the Kruskal-Wallis test with Dunn's post hoc correction (for multiple groups). *IGHV*, immunoglobulin heavy-chain variable gene; U-IGHV, unmutated IGHV; M-IGHV, mutated IGHV; ZAP-70, zeta-chain-associated protein kinase 70; CLL, chronic lymphocytic leukemia; Gal-9, Galectin-9.

crucial in CLL pathogenesis, patient outcomes, and therapeutic strategies [46,47].

The overproduction of Gal-9 has been shown to have deleterious immunosuppressive effects in multiple malignant diseases. In solid tumors and hematological malignancies, the presence of Gal-9 expression is associated with poor prognosis [6,8,20,48]. A significant increase in Gal-9 expression was seen in patients with acute myeloid leukemia who had not responded to treatment [49,50]. In recent studies, it has been suggested that changes in Gal-9 expression in malignant B-cells could be a valuable clinical indicator for monitoring CLL progression and evaluating treatment outcomes [21,51,52]. According to Taghiloo *et al.* [40], the poor prognosis of CLL patients was caused by the upregulation of Gal-9. In our investigation, it was discovered that CLL patients who needed therapy had a significantly higher level of Gal-9 concentration and $CD19^+$/Gal-9^+ cells at the time of diagnosis than those who were not treated during the period of observation. The current study found that the percentage of Gal-9 positive B cells may be a potential, independent prognostic factor for time to first treatment (TTFT) in CLL patients, which is a significant finding. Thus, it may suggest that predicting the prognosis of CLL patients could be aided by including the percentage of Gal-9^+ B cells. It is worth mentioning that several prognostic markers, which reflect the biological behavior of the CLL clone, are assessed by flow cytometry [44,53]. The best established of the flow-cytometry based markers are CD38, ZAP-70, and CD49d. They influence the course of the disease and lead to a decrease in time to treatment and overall survival [44,45,53]. Although there is controversy surrounding their clinical utility [44,54], these mark-

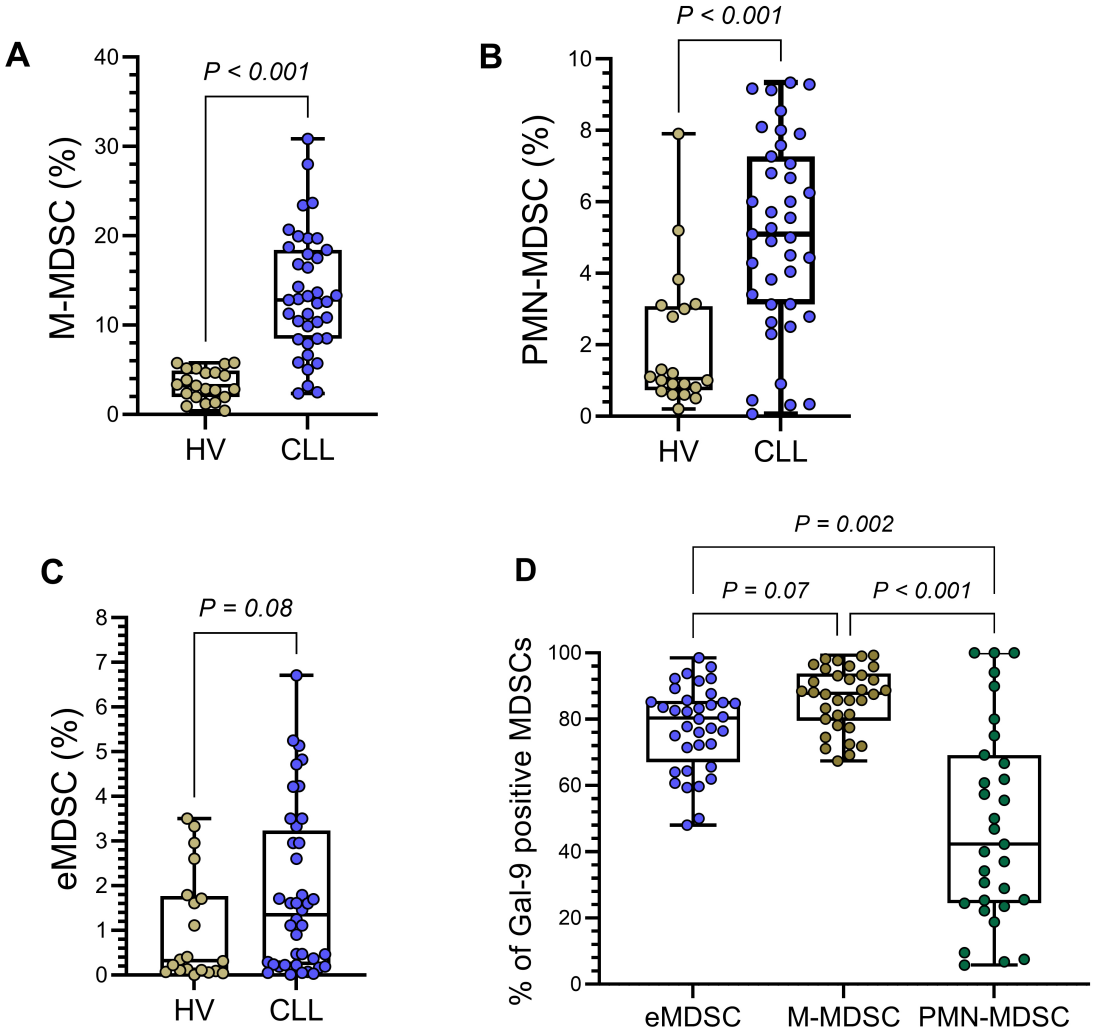

Fig. 6. Frequency of MDSC subpopulations and expression levels of Gal-9 in each subset. (A–C) MDSC subpopulations percentage in peripheral blood of 40 CLL patients compared to 20 healthy volunteers (HVs). (A) M-MDSC (monocytic, $CD14^{+}HLA\text{-}DR^{low/-}CD15$-); (B) PMN-MDSC (polymorphonuclear, $CD11b^{+}CD14^{-}CD15^{+}$); (C) eMDSC (early-stage, $Lin^{-}HLA\text{-}DR^{low/-}CD11b^{+}CD33^{+}$); (D) Gal-9 expression was calculated among M-MDSC, PMN-MDSC, and eMDSC *p*-values were calculated using the Mann-Whitney U test (for two-group comparisons) or the Kruskal-Wallis test with Dunn's post hoc correction (for multiple groups). HLA, human leukocyte antigen; MDSC, myeloid-derived suppressor cells.

ers are essential for understanding the pathobiology of the disease. Moreover, the assessment of membrane expression of various antigens by flow cytometry is highly preferred by clinicians due to its simplicity and convenience [45]. This begs the question of whether the membrane expression of Gal-9 can be a potential biomarker in CLL. Despite the uncertainty of the data, there's a convincing suggestion that elevated expression of Gal-9 in CLL is connected to several negative prognostic factors and a short time to initiation of first treatment. Nevertheless, further studies are still needed, such as whether Gal-9 expression may vary during the course of the disease.

So, what is the cause of Gal-9's poor prognosis? Gal-9 is a protein that is produced and secreted by different cell types. Its expression has been detected in tumor cells and other cells in TME, such as monocytes, dendritic cells, lymphocytes, and non-immune cells. Gal-9 can be found both in the extracellular and intracellular compartments [8,52]. Serum Gal-9 levels may increase significantly as a result of an increase in cancer cell proliferation and cellular or tissue damage [2]. Bozorgmehr *et al.* [51] stated that the shedding of Gal-9 from leukemic B cells caused a rise in plasma Gal-9 levels in CLL patients. CLL cells are the major source of Gal-9 when compared to their non-malignant counterparts. Our research seems to confirm their reports, as we have shown a positive correlation between plasma Gal-9 concentration and the percentage of B cells with Gal-9 expression. It is worth noting that Gal-9 has been identified as a protein having distinct functions for intracellular, cell surface, and extracellular areas [55]. Intracellular and cell surface Gal-9

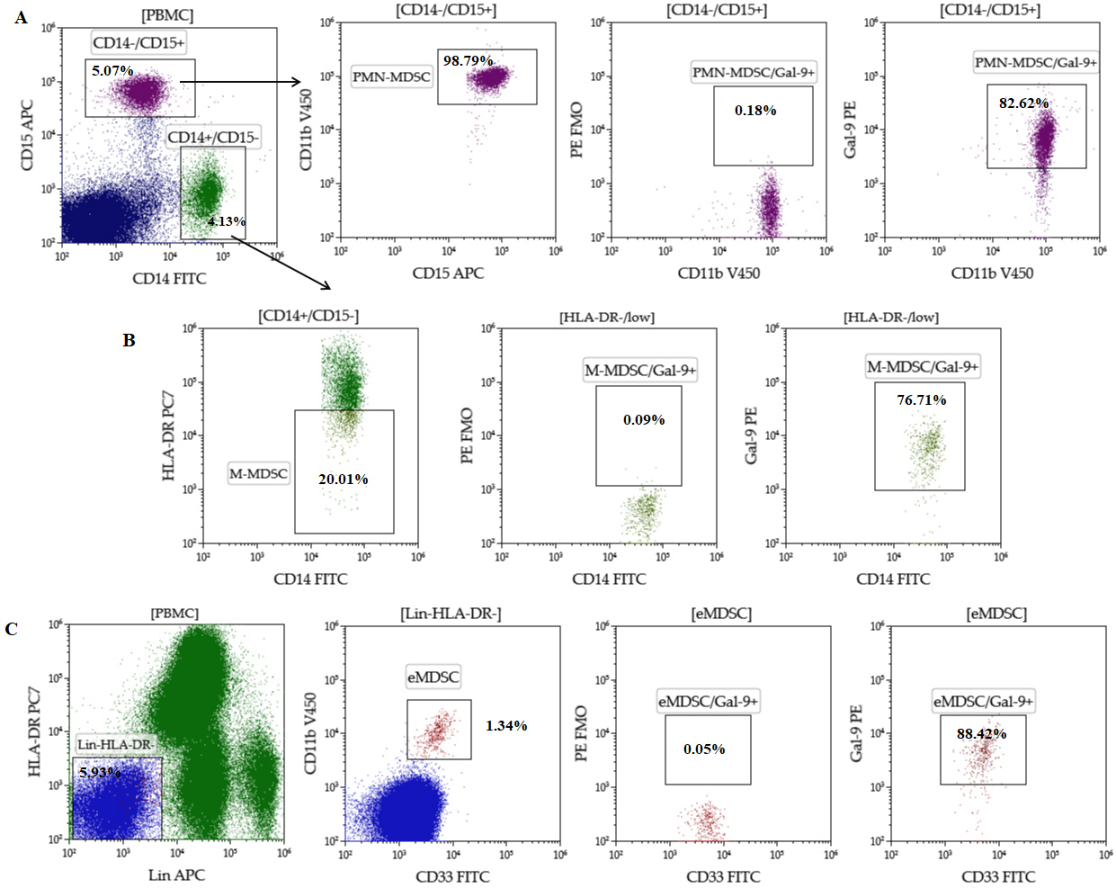

Fig. 7. The gating strategy for the identification of MDSC subsets with Gal-9 expression. Doublets were excluded, and PBMCs were gated (as shown in Fig. 3). $CD14^{-}CD11b^{+}CD15^{+}$ (PMN-MDSC, (A)), $CD14^{+}HLA\text{-}DR^{low/-}CD15^{-}$ (M-MDSC, (B)), and $Lin^{-}HLA^{-}DR^{low/-}CD11b^{+}CD33^{+}$ (eMDSC, (C)) were evaluated. In each subpopulation, the expression of Gal-9 was assessed. Each dot plot's title displays the input gate. Fluorescent minus one (FMO) controls were used to set the gating. Kaluza 2.1.1 software (Beckman Coulter, Brea, CA, USA) was employed for data analysis. PBMC, peripheral blood mononuclear cells; MDSC, myeloid-derived suppressor cells; PMN-MDSC, polymorphonuclear MDSC; M-MDSC, monocytic MDSC; eMDSC, early-stage MDSC; Gal-9, Galectin-9.

have an impact on cell signaling. Cell surface Gal-9 is a crucial component in the interaction between neighboring cells and the adhesion to the extracellular matrix. When Gal-9 is released, it acts like an immunomodulatory cytokine [55]. Gal-9 is essentially an inhibitor of the immune system. It has an effect on the expansion of regulatory T cells (Tregs) and enhances their immunosuppressive capacity. It has been demonstrated that Gal-9 reduces Th17 and Th1 cells. Gal-9 also induces apoptosis of $CD8^{+}$ cytotoxic cells [2]. It's worth mentioning that it has also been implicated in the expansion of MDSCs [16,55]. In our study, we decided to identify MDSC subsets and perform Gal-9 staining in this population. To the best of our knowledge, we are the first to correlate three MDSC subpopulations, monocytic (M-MDSC), polymorphonuclear (PMN-MDSC), and early-stage (eMDSC) expressing Gal-9 with the plasma concentration of this protein. As we have already mentioned, we confirmed our previous findings [24] that M-MDSCs are significantly increased in CLL patients compared to healthy volunteers. Additionally, in the CLL patients PMN-MDSC subpopulation was significantly higher than in healthy controls. Likewise, the percentage of subpopulations with the eMDSC phenotype was higher in patients with CLL. Despite this, the difference was not statistically significant. The plasma levels of Gal-9 were closely linked to the percentages of eMDSC/Gal-9^{+} and M-MDSC/Gal-9^{+}. It appears that Gal-9 concentration can be significantly elevated not only due to an increase in cancer cell proliferation, but also due to a boost in MDSC cells. Gal-9's over-circulating state competes for receptors outside its cellular environment, including TIM-3 or PD-1, which can lead to unwanted signals like immunosuppression [2]. Moreover, TIM-3/Gal-9 interactions could induce the proliferation of MDSCs, which in turn suppressed proliferation and activation of T-cell [56].

Interestingly, Gal-9 has been found to be responsible for tumor or viral immunity evasion in nasopharyngeal carcinoma related to Epstein-Barr virus (EBV) [57,58]. Our

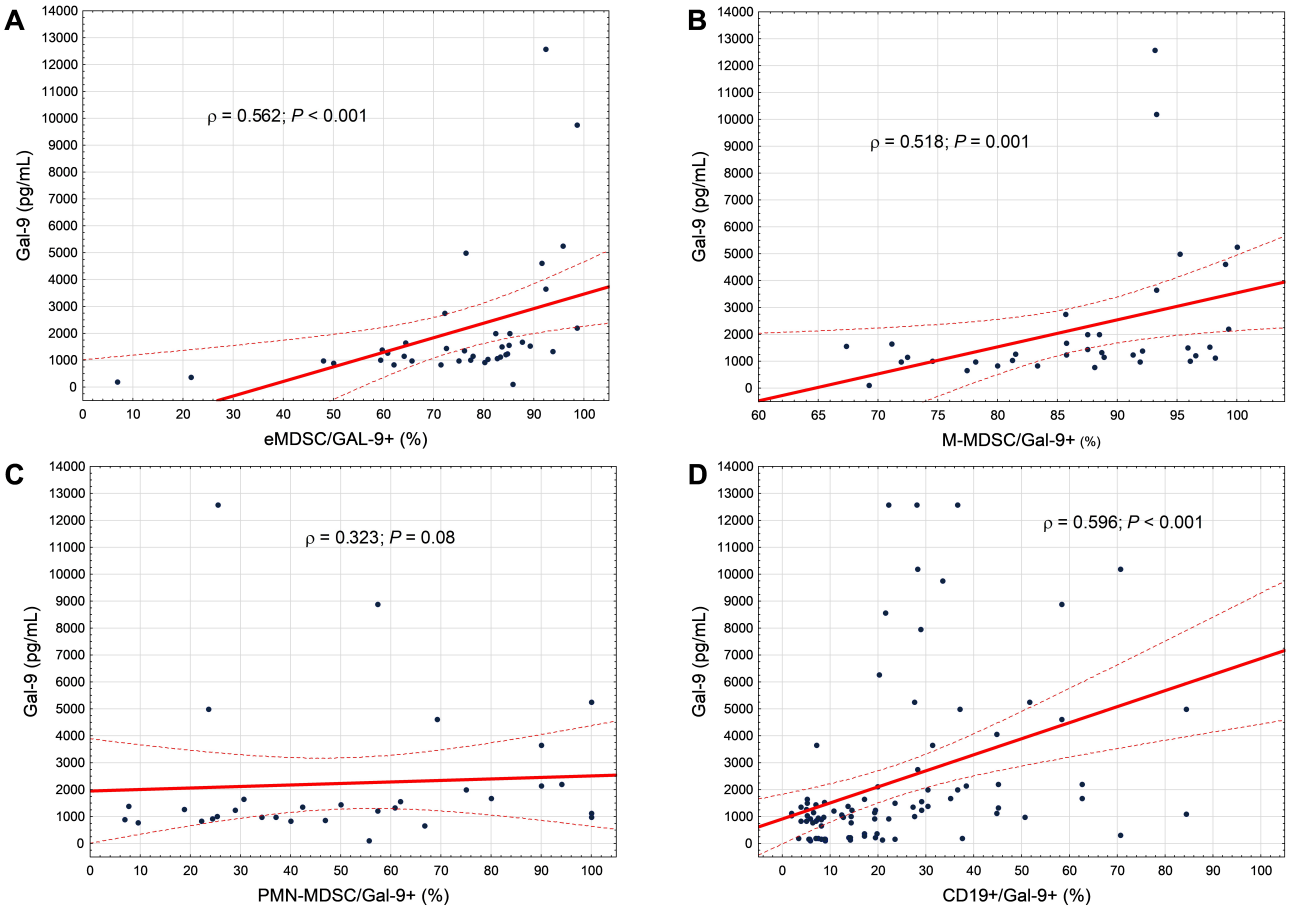

Fig. 8. Gal-9 plasma levels correlation with Gal-9-positive MDSCs and B-cells. (A) The correlation between the Gal-9 plasma level and eMDSC/Gal-9$^+$ percentage. (B) The correlation between the M-MDSC/Gal-9$^+$ and Gal-9 plasma level. (C) The association between the percentage of PMN-MDSC/Gal-9$^+$ and Gal-9 plasma level. (D) The positive correlation of the CD19$^+$/Gal-9$^+$ cell percentage with the plasma concentration of Gal-9. ρ, Spearman's rank correlation coefficient; MDSC, myeloid-derived suppressor cells; PMN-MDSC, polymorphonuclear MDSC; M-MDSC, monocytic MDSC; eMDSC, early-stage MDSC; Gal-9, Galectin-9.

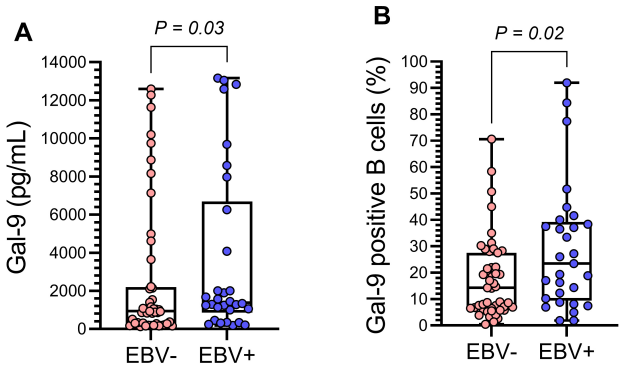

Fig. 9. The association between Gal-9 expression and EBV status. Gal-9 plasma concentration (A) and the percentage of B cells with Gal-9 expression (B) in EBV-negative (EBV-) and EBV-positive (EBV+) CLL patients. *p*-values were calculated using the Mann-Whitney U test. EBV, Epstein-Barr virus; Gal-9, Galectin-9.

research focused on the relationship between Gal-9 expression and EBV status of CLL patients. The role of EBV in CLL aetiology was widely studied [29,59,60]. Visco *et al.* [59] revealed that the EBV DNA load in patients with CLL strongly correlated with overall survival. Furthermore, CLL patients were found to have a significantly reduced time to treatment if they were EBV+ [59,60]. Our study revealed that EBV-positive CLL cases had a significantly higher plasma Gal-9 concentration and percentage of B cells with Gal-9 expression. It is worth paying attention to the study of Xu and colleagues [26] who observed an enduring increase in the expression of *Gal-9* mRNA using an experimental model that involved EBV transformation of B cells. Moreover, the addition of exogenous recombinant Gal-9 promoted the outgrowth of EBV-infected B cells and the establishment of the acute/latent infection phases [26]. In our study of CLL patients who had a positive EBV-DNA test, we found a significant relationship between the EBV-DNA copy number and the percentage of B cells that expressed Gal-9.

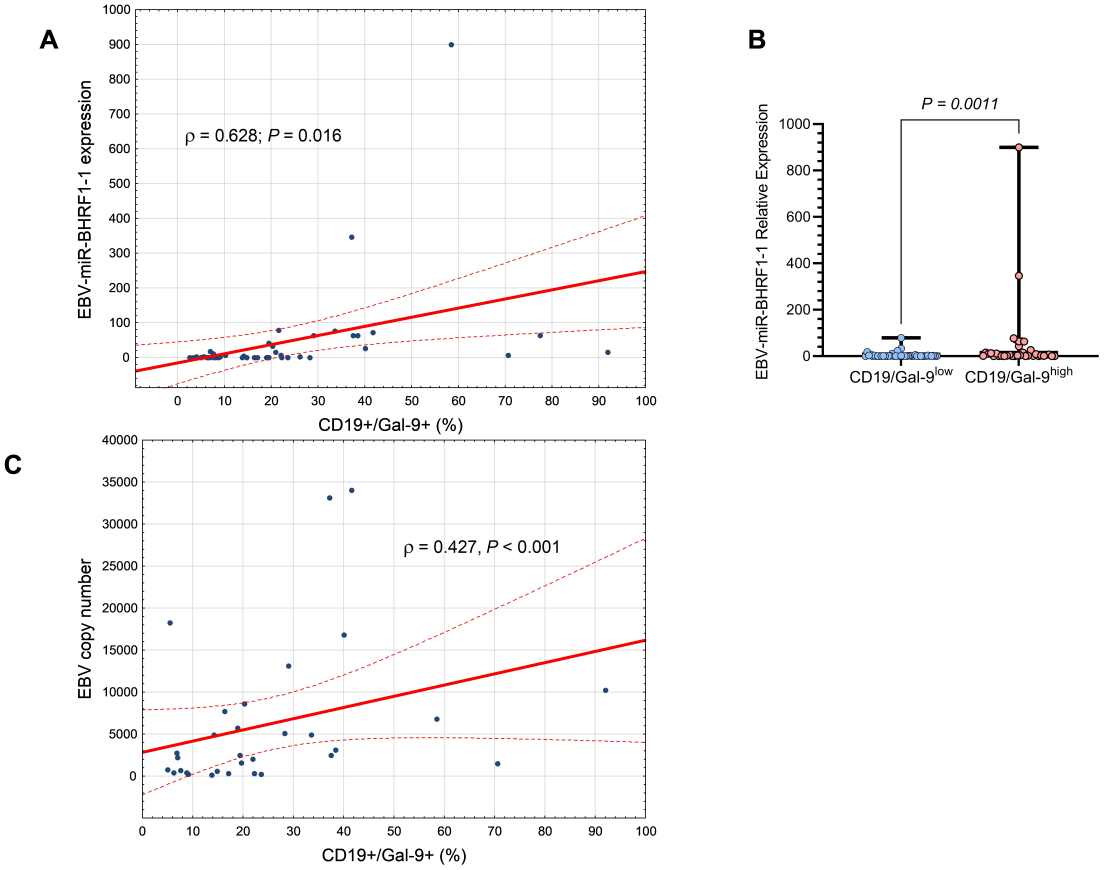

Fig. 10. The association between Gal-9 and EBV-miR-BHRF1-1 expression and EBV copy number. (A) The percentage of $CD19^+/Gal\text{-}9^+$ cells was correlated with the expression of EBV-miR-BHRF1-1 in CLL cells. (B) Using 28.03% as a cut-off, CLL patients were divided into two groups: $CD19/Gal\text{-}9^{low}$ (less than 28.03% $Gal\text{-}9^+/CD19^+$ cells) and $CD19/Gal\text{-}9^{high}$ (28.03% or more $Gal\text{-}9^+CD19^+$ cells). The cut-point for the percentage of $Gal\text{-}9^+/CD19^+$ cells was chosen based on the receiver operating characteristics (ROC) analysis. EBV-miR-BHRF1-1 expression in the $CD19/Gal\text{-}9^{high}$ group was compared to that of the $CD19/Gal\text{-}9^{low}$ group. (C) The correlation between the EBV-DNA copy number and the percentage of Gal-9-positive B cells. *p*-value was calculated using the Mann-Whitney U test. EBV, Epstein-Barr virus; BHRF1-1, BamH1 fragment H rightward facing 1-1; Gal-9, Galectin-9.

In EBV, 44 mature microRNAs have been identified that can be classified into two clusters (BHRF1 and BamHI-A Rightward Transcripts (BART)). The expression of BHRF1 miRNA is significant at stage III latency, while BART miRNAs are present in every EBV-positive cell line [26,61–63]. According to Xu *et al.* [29], EBV-DNA-positive CLL patients expressed higher levels of EBV-BHRF1-1 than EBV-DNA-negative ones in leukemic B cells. EBV-miR-BHRF1-1 in the study of Xu *et al.* [29] has been detected in EBV-positive CLL patients. They proposed that EBV-positive CLL may be classified as a stage III form of latency, a condition characterized by the expression of latent genes and the presence of both EBV miRNA clusters (BHRF1 and BART) [29]. Moreover, they showed that patients with higher expression of EBV-BHRF1-1 were more likely to have shorter time to treatment and lower overall survival [29]. In our study, EBV-miRBHRF1-1 expression of CLL patients was analyzed for association with the percentage of B cells with Gal-9 expression. The expression levels of EBV-miR-BHRF1-1 in CLL patients were positively correlated with the percentage of $Gal\text{-}9^+$ B cells. In addition, we analyzed the EBV-miR-BHRF1-1 expression in CLL by splitting our cohort based on the cut-off for $CD19^+/Gal\text{-}9^+$ percentage into high and low. We found a significant increase of EBV-miR-BHRF1-1 in the $CD19/Gal\text{-}9^{high}$ group.

It is worth pointing out that B cells transformed by EBV latency III have an immunoregulatory potential. The expression of immunosuppressive molecules such as IL-10 and PD-L1 characterized these cells. Both markers are characteristics of regulatory B cells. Considering that EBV latency III B cells display an immunosuppressive profile similar to Breg [36], we analyzed the association of B cells with surface Gal-9 expression with the Breg phenotype ($CD19^+CD24^{high}CD38^{high}$). We noted that Gal-9 expression was significantly higher within the $CD19^+CD5^+CD24^{high}CD38^{high}$ fraction of CLL cells (Breg) relative to the $CD19^+CD5^+CD24^+CD38^{low}$ frac-

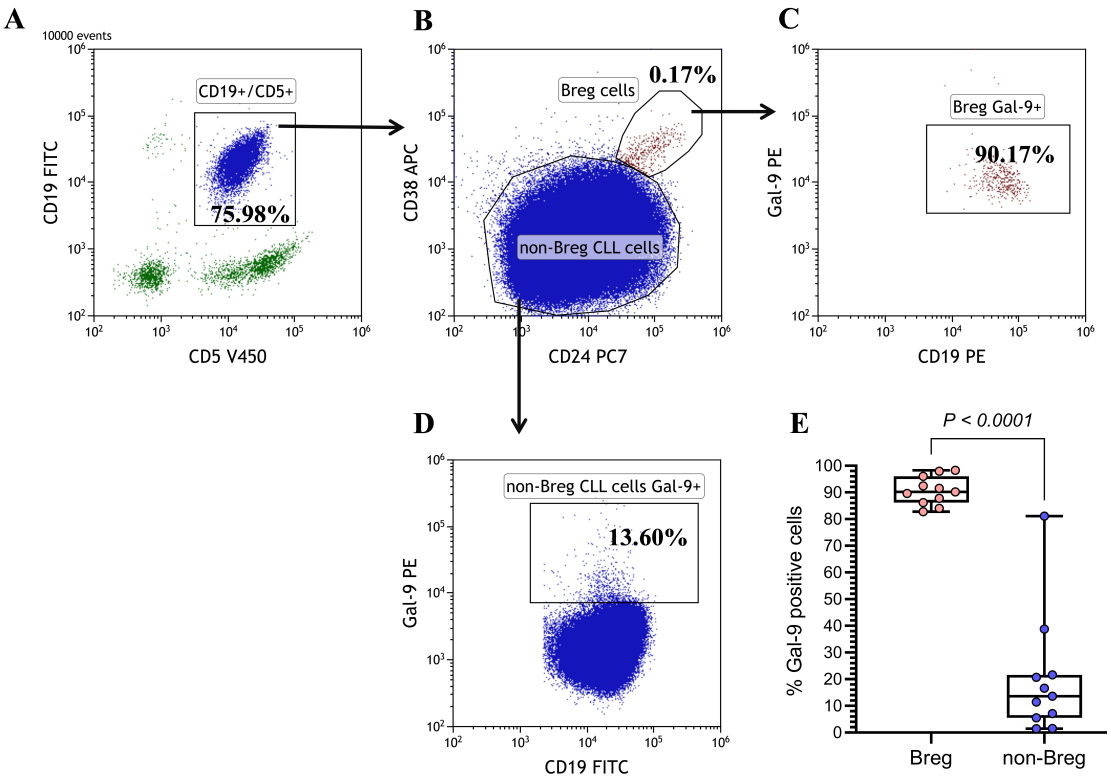

Fig. 11. Gal-9-expressing B cells exhibit the Breg phenotype. (A,B) Gating strategy of Breg. Flow cytometry analysis of the $CD19^{+}CD5^{+}CD24^{high}CD38^{high}$ cells was performed among $CD19^{+}CD5^{+}$ B cells. (C) It was noted that Gal-9 expression was significantly higher within the $CD19^{+}CD5^{+}CD24^{high}CD38^{high}$ fraction (Breg CLL cells) in comparison to (D) the $CD19^{+}CD5^{-}CD24^{+}CD38^{low}$ fraction (non-Breg CLL cells). (E) Percentage of Gal-9 positive cells within the $CD19^{+}CD5^{+}CD24^{high}CD38^{high}$ Breg and non-Breg CLL cells ($CD19^{+}CD5^{-}CD24^{+}CD38^{low}$) from 11 CLL patients. Kaluza 2.1.1 software (Beckman Coulter, Brea, CA, USA) was employed for data analysis. *p*-value was calculated using the Mann-Whitney U test. Breg, B regulatory cell.

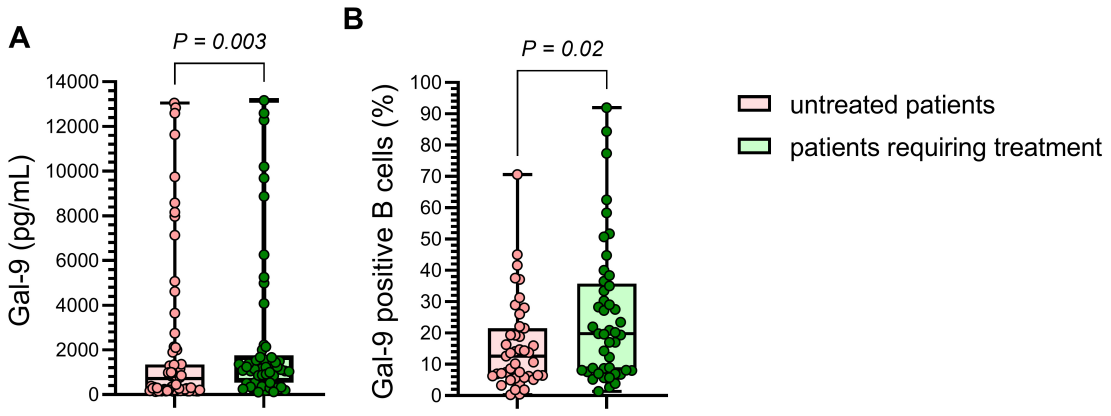

Fig. 12. Comparison of Gal-9 in patients requiring therapy compared to those who do not require treatment. (A) Plasma concentrations of Gal-9. (B) Percentage of B cells positive for Gal-9. *p*-values were calculated using the Mann-Whitney U test.

tion (non-Breg CLL cells). Research on B cells with regulatory abilities has shown that Breg and CLL cells have significant similarities [64–66]. Based on Gal-9's immunoregulatory role [67], we can speculate that Gal-9 could increase the immunosuppressive potential of Breg.

Conclusions

Our study's data revealed that an increase in cancer cell production and a boost in MDSC cells can cause a significant increase in Gal-9 concentration. Moreover, higher concentrations of Gal-9 and percentages of $CD19^{+}$/Gal-

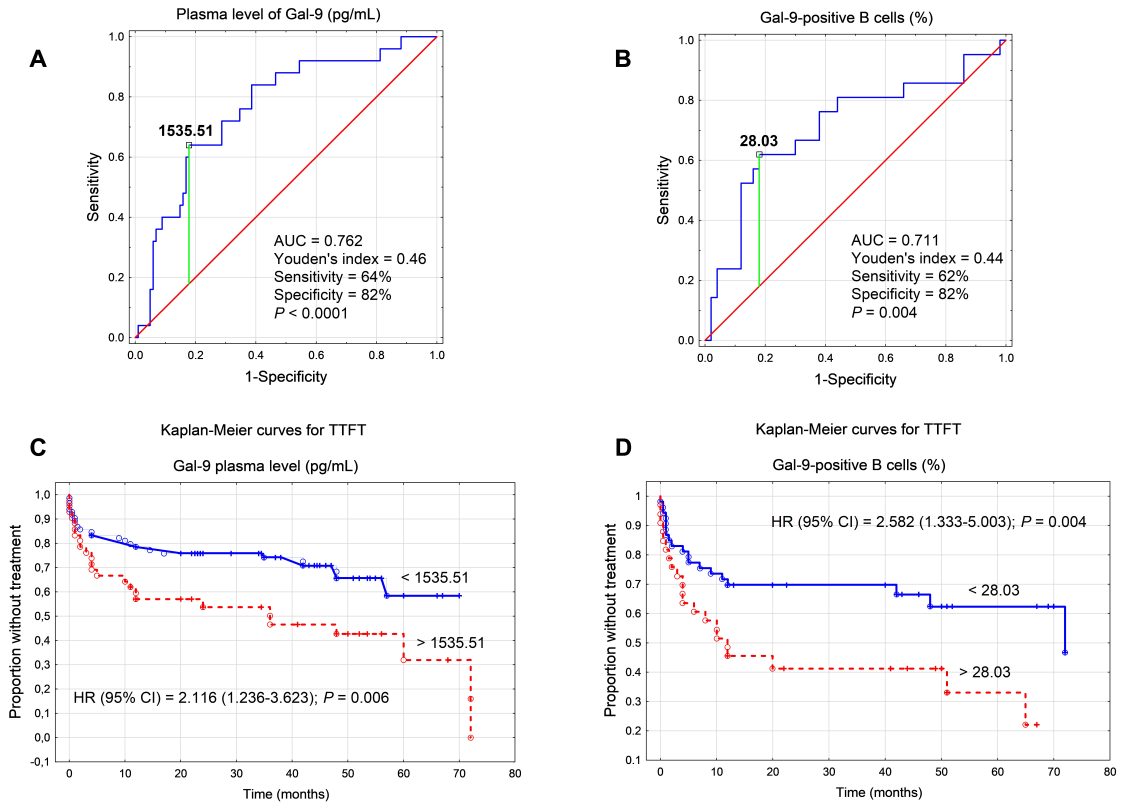

Fig. 13. Prognostic significance of Galectin-9 expression in CLL patients. (A) The optimal cut-point values for plasma Gal-9 concentration and (B) percentage of Gal-9-positive B cells were chosen using receiver operating characteristics (ROC) curves. The Youden Index was applied to select the threshold that maximized sensitivity and specificity. Kaplan-Meier survival curves for time to first treatment (TTFT), stratified by Gal-9 plasma concentration (C,D) percentage of Gal-9-positive B cells. AUC, area under the curve; HR, hazard ratio; CI, confidence interval.

9^+ cells are linked to EBV positivity and poor clinical outcomes of CLL patients. The expression of EBV-miR-BHRF1-1, which is significant at stage III latency, positively correlates with the percentage of Gal-9-positive B cells and Gal-9 plasma concentration. Gal-9-positive CLL cells display a phenotype similar to B regulatory cells. It is therefore possible that Gal-9's immunoregulatory function may lead to a boost in Breg immunosuppressive potential.

Availability of Data and Materials

The authors declare that all relevant data of this study are available within the article or from the corresponding author on reasonable request.

Author Contributions

ABJ and PP conceptualized and designed the study; PP, AS, SC, MZ, JW, WT, JR, and ABJ performed the research. PP, AS, SC, MZ, JW, WT, JR, and ABJ contributed to data acquisition. PP and ABJ analyzed and interpreted data for the work. JR, MZ, and ABJ provided help and advice on the research study. PP and ABJ have been involved in drafting the manuscript, and all authors have been involved in revising it critically for important intellectual content. All authors contributed to editorial changes in the manuscript. All authors read and approved the final manuscript. All authors have participated sufficiently in the work and agreed to be accountable for all aspects of the work.

Ethics Approval and Consent to Participate

The study was conducted according to the guidelines of the Declaration of Helsinki and approved by the Ethics Committee of the Medical University of Lublin No. KE-0254/88/2016 (date of approval: 24 March 2016), KE-0254/6/2020 (date of approval: 28 January 2020), and KE-0254/186/10/2022 (date of approval: 6 October 2022). Written informed consent was obtained from all patients.

Acknowledgment

We are thankful to Maciej Maj from the Department of Biopharmacy, Medical University of Lublin, Poland for his technical assistance in preparing confocal microscopy images.

Funding

This work was supported by the Medical University of Lublin, Poland (grant numbers DS 458, DS 461).

Conflict of Interest

The authors declare no conflict of interest. Agnieszka Bojarska-Junak serves as one of the editorial board members of this journal. We declare that Agnieszka Bojarska-Junak had no involvement in the peer review of this article and has no access to information regarding its peer review.

References

[1] Yang R, Sun L, Li CF, Wang YH, Yao J, Li H, *et al*. Galectin-9 interacts with PD-1 and TIM-3 to regulate T cell death and is a target for cancer immunotherapy. Nature Communications. 2021; 12: 832. https://doi.org/10.1038/s41467-021-21099-2.

[2] Lv Y, Ma X, Ma Y, Du Y, Feng J. A new emerging target in cancer immunotherapy: Galectin-9 (LGALS9). Genes & Diseases. 2022; 10: 2366–2382. https://doi.org/10.1016/j.gendis.2022.05.020.

[3] Yıldırım C. Galectin-9, a pro-survival factor inducing immunosuppression, leukemic cell transformation and expansion. Molecular Biology Reports. 2024; 51: 571. https://doi.org/10.1007/s11033-024-09563-w.

[4] Liu FT, Stowell SR. The role of galectins in immunity and infection. Nature Reviews. Immunology. 2023; 23: 479–494. https://doi.org/10.1038/s41577-022-00829-7.

[5] Rezaei M, Ghanadian M, Ghezelbash B, Shokouhi A, Bazhin AV, Zamyatnin AA, Jr, *et al*. TIM-3/Gal-9 interaction affects glucose and lipid metabolism in acute myeloid leukemia cell lines. Frontiers in Immunology. 2023; 14: 1267578. https://doi.org/10.3389/fimmu.2023.1267578.

[6] Zheng Y, Feng W, Wang YJ, Sun Y, Shi G, Yu Q. Galectins as potential emerging key targets in different types of leukemia. European Journal of Pharmacology. 2019; 844: 73–78. https://doi.org/10.1016/j.ejphar.2018.11.019.

[7] Bailly C, Thuru X, Quesnel B. Modulation of the Gal-9/TIM-3 Immune Checkpoint with α-Lactose. Does Anomery of Lactose Matter? Cancers. 2021; 13: 6365. https://doi.org/10.3390/cancers13246365.

[8] Moar P, Tandon R. Galectin-9 as a biomarker of disease severity. Cellular Immunology. 2021; 361: 104287. https://doi.org/10.1016/j.cellimm.2021.104287.

[9] Beyer S, Wehrmann M, Meister S, Kolben TM, Trillsch F, Burges A, *et al*. Galectin-8 and -9 as prognostic factors for cervical cancer. Archives of Gynecology and Obstetrics. 2022; 306: 1211–1220. https://doi.org/10.1007/s00404-022-06449-9.

[10] Ustyanovska Avtenyuk N, Choukrani G, Ammatuna E, Niki T, Cendrowicz E, Lourens HJ, *et al*. Galectin-9 Triggers Neutrophil-Mediated Anticancer Immunity. Biomedicines. 2021; 10: 66. https://doi.org/10.3390/biomedicines10010066.

[11] Rahmati A, Bigam S, Elahi S. Galectin-9 promotes natural killer cells activity *via* interaction with CD44. Frontiers in Immunology. 2023; 14: 1131379. https://doi.org/10.3389/fimmu.2023.1131379.

[12] Tao J, Han D, Gao S, Zhang W, Yu H, Liu P, *et al*. $CD8^+$ T cells exhaustion induced by myeloid-derived suppressor cells in myelodysplastic syndromes patients might be through TIM3/Gal-9 pathway. Journal of Cellular and Molecular Medicine. 2020; 24: 1046–1058. https://doi.org/10.1111/jcmm.14825.

[13] Matsumoto H, Fujita Y, Matsuoka N, Temmoku J, Yashiro-Furuya M, Asano T, *et al*. Serum checkpoint molecules in patients with IgG4-related disease (IgG4-RD). Arthritis Research & Therapy. 2021; 23: 148. https://doi.org/10.1186/s13075-021-02527-6.

[14] Tadokoro T, Fujihara S, Chiyo T, Oura K, Samukawa E, Yamana Y, *et al*. Induction of apoptosis by Galectin-9 in liver metastatic cancer cells: In vitro study. International Journal of Oncology. 2017; 51: 607–614. https://doi.org/10.3892/ijo.2017.4053.

[15] Sauer N, Janicka N, Szlasa W, Skinderowicz B, Kołodzińska K, Dwernicka W, *et al*. TIM-3 as a promising target for cancer immunotherapy in a wide range of tumors. Cancer Immunology, Immunotherapy: CII. 2023; 72: 3405–3425. https://doi.org/10.1007/s00262-023-03516-1.

[16] Zhang CX, Huang DJ, Baloche V, Zhang L, Xu JX, Li BW, *et al*. Galectin-9 promotes a suppressive microenvironment in human cancer by enhancing STING degradation. Oncogenesis. 2020; 9: 65. https://doi.org/10.1038/s41389-020-00248-0.

[17] Wang K, Chen Z, Wu R, Yin J, Fan M, Xu X. Prognostic Role of High Gal-9 Expression in Solid Tumours: a Meta-Analysis. Cellular Physiology and Biochemistry: International Journal of Experimental Cellular Physiology, Biochemistry, and Pharmacology. 2018; 45: 993–1002. https://doi.org/10.1159/000487294.

[18] Zhou X, Sun L, Jing D, Xu G, Zhang J, Lin L, *et al*. Galectin-9 Expression Predicts Favorable Clinical Outcome in Solid Tumors: A Systematic Review and Meta-Analysis. Frontiers in Physiology. 2018; 9: 452. https://doi.org/10.3389/fphys.2018.00452.

[19] Okoye I, Xu L, Motamedi M, Parashar P, Walker JW, Elahi S. Galectin-9 expression defines exhausted T cells and impaired cytotoxic NK cells in patients with virus-associated solid tumors. Journal for Immunotherapy of Cancer. 2020; 8: e001849. https://doi.org/10.1136/jitc-2020-001849.

[20] Giordano M, Croci DO, Rabinovich GA. Galectins in hematological malignancies. Current Opinion in Hematology. 2013; 20: 327–335. https://doi.org/10.1097/MOH.0b013e328362370f.

[21] Wdowiak K, Gallego-Colon E, Francuz T, Czajka-Francuz P, Ruiz-Agamez N, Kubeczko M, *et al*. Increased serum levels of Galectin-9 in patients with chronic lymphocytic leukemia. Oncology Letters. 2019; 17: 1019–1029. https://doi.org/10.3892/ol.2018.9656.

[22] Alimu X, Zhang J, Pang N, Zhang R, Chen R, Zeng X, *et al*. Galectin-9 and myeloid-derived suppressor cell as prognostic indicators for chronic lymphocytic leukemia. Immunity, Inflammation and Disease. 2023; 11: e853. https://doi.org/10.1002/iid3.853.

[23] Bojarska-Junak A, Kowalska W, Chocholska S, Szymańska A, Tomczak W, Zarobkiewicz MK, *et al*. Prognostic Potential of Galectin-9 mRNA Expression in Chronic Lymphocytic Leukemia. Cancers. 2023; 15: 5370. https://doi.org/10.3390/cancers15225370.

[24] Zarobkiewicz M, Kowalska W, Chocholska S, Tomczak W, Szymańska A, Morawska I, *et al*. High M-MDSC Percentage as a Negative Prognostic Factor in Chronic Lymphocytic Leukaemia. Cancers. 2020; 12: 2614. https://doi.org/10.3390/cancers12092614.

[25] Ferrer G, Jung B, Chiu PY, Aslam R, Palacios F, Mazzarello AN, *et al*. Myeloid-derived suppressor cell subtypes differentially influence T-cell function, T-helper subset differentiation, and clinical course in CLL. Leukemia. 2021; 35: 3163–3175. https://doi.org/10.1038/s41375-021-01249-7.

[26] Xu JX, Zhang R, Huang DJ, Tang Y, Ping LQ, Huang BJ, *et al*. Galectin-9 Facilitates Epstein-Barr Virus Latent Infection and Lymphomagenesis in Human B Cells. Microbiology Spectrum. 2023; 11: e0493222. https://doi.org/10.1128/spectrum.04932-22.

[27] Giovannone N, Liang J, Antonopoulos A, Geddes Sweeney J, King SL, Pochebit SM, *et al*. Galectin-9 suppresses B cell receptor signaling and is regulated by I-branching of N-glycans. Nature Communications. 2018; 9: 3287. https://doi.org/10.1038/s41467-018-05770-9.

[28] Xing L, Kieff E. Epstein-Barr virus BHRF1 micro- and stable RNAs during latency III and after induction of replication. Journal of Virology. 2007; 81: 9967–9975. https://doi.org/10.1128/JVI.02244-06.

[29] Xu DM, Kong YL, Wang L, Zhu HY, Wu JZ, Xia Y, *et al*. EBV-miR-BHRF1-1 Targets p53 Gene: Potential Role in Epstein-Barr Virus Associated Chronic Lymphocytic Leukemia. Cancer Research and Treatment. 2020; 52: 492–504. https://doi.org/10.4143/crt.2019.457.

[30] Hallek M, Cheson BD, Catovsky D, Caligaris-Cappio F, Dighiero G, Döhner H, *et al*. iwCLL guidelines for diagnosis, indications for treatment, response assessment, and supportive management of CLL. Blood. 2018; 131: 2745–2760. https://doi.org/10.1182/blood-2017-09-806398.

[31] Rai KR, Sawitsky A, Cronkite EP, Chanana AD, Levy RN, Pasternack BS. Clinical staging of chronic lymphocytic leukemia. Blood. 1975;46(2):219-234. Blood. 2016; 128: 2109. https://doi.org/10.1182/blood-2016-08-737650.

[32] Bronte V, Brandau S, Chen SH, Colombo MP, Frey AB, Greten TF, *et al*. Recommendations for myeloid-derived suppressor cell nomenclature and characterization standards. Nature Communications. 2016; 7: 12150. https://doi.org/10.1038/ncomms12150.

[33] Hus I, Podhorecka M, Bojarska-Junak A, Roliński J, Schmitt M, Sieklucka M, *et al*. The clinical significance of ZAP-70 and CD38 expression in B-cell chronic lymphocytic leukaemia. Annals of Oncology: Official Journal of the European Society for Medical Oncology. 2006; 17: 683–690. https://doi.org/10.1093/annonc/mdj120.

[34] Woś J, Chocholska S, Kowalska W, Tomczak W, Szymańska A, Karczmarczyk A, *et al*. Prognostic Value of Tie2-Expressing Monocytes in Chronic Lymphocytic Leukemia Patients. Cancers. 2021; 13: 2817. https://doi.org/10.3390/cancers13112817.

[35] Chocholska S, Zarobkiewicz M, Szymańska A, Lehman N, Woś J, Bojarska-Junak A. Prognostic Value of the miR-17 92 Cluster in Chronic Lymphocytic Leukemia. International Journal of Molecular Sciences. 2023; 24: 1705. https://doi.org/10.3390/ijms24021705.

[36] Auclair H, Ouk-Martin C, Roland L, Santa P, Al Mohamad H, Faumont N, *et al*. EBV Latency III-Transformed B Cells Are Inducers of Conventional and Unconventional Regulatory T Cells in a PD-L1-Dependent Manner. Journal of Immunology (Baltimore, Md.: 1950). 2019; 203: 1665–1674. https://doi.org/10.4049/jimmunol.1801420.

[37] Burger JA, Gribben JG. The microenvironment in chronic lymphocytic leukemia (CLL) and other B cell malignancies: insight into disease biology and new targeted therapies. Seminars in Cancer Biology. 2014; 24: 71–81. https://doi.org/10.1016/j.semcancer.2013.08.011.

[38] Taghiloo S, Asgarian-Omran H. Current Approaches of Immune Checkpoint Therapy in Chronic Lymphocytic Leukemia. Current Treatment Options in Oncology. 2023; 24: 1408–1438. https://doi.org/10.1007/s11864-023-01129-5.

[39] Pang N, Alimu X, Chen R, Muhashi M, Ma J, Chen G, *et al*. Activated Galectin-9/Tim3 promotes Treg and suppresses Th1 effector function in chronic lymphocytic leukemia. FASEB Journal: Official Publication of the Federation of American Societies for Experimental Biology. 2021; 35: e21556. https://doi.org/10.1096/fj.202100013R.

[40] Taghiloo S, Allahmoradi E, Ebadi R, Tehrani M, Hosseini-Khah Z, Janbabaei G, *et al*. Upregulation of Galectin-9 and PD-L1 Immune Checkpoints Molecules in Patients with Chronic Lymphocytic Leukemia. Asian Pacific Journal of Cancer Prevention: APJCP. 2017; 18: 2269–2274. https://doi.org/10.22034/APJCP.2017.18.8.2269.

[41] Hampel PJ, Parikh SA. Chronic lymphocytic leukemia treatment algorithm 2022. Blood Cancer Journal. 2022; 12: 161. https://doi.org/10.1038/s41408-022-00756-9.

[42] Paulus A, Malavasi F, Chanan-Khan A. CD38 as a multifaceted immunotherapeutic target in CLL. Leukemia & Lymphoma. 2022; 63: 2265–2275. https://doi.org/10.1080/10428194.2022.2090551.

[43] Eichhorst B, Hallek M. Prognostication of chronic lymphocytic leukemia in the era of new agents. Hematology. American Society of Hematology. Education Program. 2016; 2016: 149–155. https://doi.org/10.1182/asheducation-2016.1.149.

[44] Cohen JA, Bomben R, Pozzo F, Tissino E, Härzschel A, Hartmann TN, *et al*. An Updated Perspective on Current Prognostic and Predictive Biomarkers in Chronic Lymphocytic Leukemia in the Context of Chemoimmunotherapy and Novel Targeted Therapy. Cancers. 2020; 12: 894. https://doi.org/10.3390/cancers12040894.

[45] Amaya-Chanaga CI, Rassenti LZ. Biomarkers in chronic lymphocytic leukemia: Clinical applications and prognostic markers. Best Practice & Research. Clinical Haematology. 2016; 29: 79–89. https://doi.org/10.1016/j.beha.2016.08.005.

[46] Puiggros A, Blanco G, Espinet B. Genetic abnormalities in chronic lymphocytic leukemia: where we are and where we go. BioMed Research International. 2014; 2014: 435983. https://doi.org/10.1155/2014/435983.

[47] Pepe F, Rassenti LZ, Pekarsky Y, Labanowska J, Nakamura T, Nigita G, *et al*. A large fraction of trisomy 12, $17p^-$, and $11q^-$ CLL cases carry unidentified microdeletions of *miR-15a/16-1*. Proceedings of the National Academy of Sciences of the United States of America. 2022; 119: e2118752119. https://doi.org/10.1073/pnas.2118752119.

[48] Fujita K, Iwama H, Oura K, Tadokoro T, Samukawa E, Sakamoto T, *et al*. Cancer Therapy Due to Apoptosis: Galectin-9. International Journal of Molecular Sciences. 2017; 18: 74. https://doi.org/10.3390/ijms18010074.

[49] Kikushige Y, Miyamoto T, Yuda J, Jabbarzadeh-Tabrizi S, Shima T, Takayanagi SI, *et al*. A TIM-3/Gal-9 Autocrine Stimulatory Loop Drives Self-Renewal of Human Myeloid Leukemia Stem Cells and Leukemic Progression. Cell Stem Cell. 2015; 17: 341–352. https://doi.org/10.1016/j.stem.2015.07.011.

[50] Zhang Y, Xue S, Hao Q, Liu F, Huang W, Wang J. Galectin-9 and PSMB8 overexpression predict unfavorable prognosis in patients with AML. Journal of Cancer. 2021; 12: 4257–4263. https://doi.org/10.7150/jca.53686.

[51] Bozorgmehr N, Hnatiuk M, Peters AC, Elahi S. Depletion of polyfunctional $CD26^{high}CD8^+$ T cells repertoire in chronic lymphocytic leukemia. Experimental Hematology & Oncology. 2023; 12: 13. https://doi.org/10.1186/s40164-023-00375-5.

[52] Liu H, Dai Q, Li Y, Tang Z, She T. Association between high galectin expression and poor prognosis in hematologic cancers: a systematic review and meta-analysis. Hematology (Amsterdam, Netherlands). 2023; 28: 2227494. https://doi.org/10.1080/16078454.2023.2227494.

[53] Varghese AM, Munir T. SOHO State of the Art Updates and Next Questions | Impact of Biologic Markers on Outcomes With Novel Therapy in Chronic Lymphocytic Leukaemia. Clinical Lymphoma, Myeloma & Leukemia. 2024; 25: 381–394. https://doi.org/10.1016/j.clml.2024.10.015.

[54] Kittai AS, Lunning M, Danilov AV. Relevance of Prognostic Factors in the Era of Targeted Therapies in CLL. Current Hematologic Malignancy Reports. 2019; 14: 302–309. https://doi.org/10.1007/s11899-019-00511-1.

[55] Lhuillier C, Barjon C, Baloche V, Niki T, Gelin A, Mustapha

R, *et al*. Characterization of neutralizing antibodies reacting with the 213-224 amino-acid segment of human galectin-9. PloS One. 2018; 13: e0202512. https://doi.org/10.1371/journal.pone.0202512.

[56] Yin J, Li L, Wang C, Zhang Y. Increased Galectin-9 expression, a prognostic biomarker of aGVHD, regulates the immune response through the Galectin-9 induced MDSC pathway after allogeneic hematopoietic stem cell transplantation. International Immunopharmacology. 2020; 88: 106929. https://doi.org/10.1016/j.intimp.2020.106929.

[57] Keryer-Bibens C, Pioche-Durieu C, Villemant C, Souquère S, Nishi N, Hirashima M, *et al*. Exosomes released by EBV-infected nasopharyngeal carcinoma cells convey the viral latent membrane protein 1 and the immunomodulatory protein galectin 9. BMC Cancer. 2006; 6: 283. https://doi.org/10.1186/1471-2407-6-283.

[58] Klibi J, Niki T, Riedel A, Pioche-Durieu C, Souquere S, Rubinstein E, *et al*. Blood diffusion and Th1-suppressive effects of galectin-9-containing exosomes released by Epstein-Barr virus-infected nasopharyngeal carcinoma cells. Blood. 2009; 113: 1957–1966. https://doi.org/10.1182/blood-2008-02-142596.

[59] Visco C, Falisi E, Young KH, Pascarella M, Perbellini O, Carli G, *et al*. Epstein-Barr virus DNA load in chronic lymphocytic leukemia is an independent predictor of clinical course and survival. Oncotarget. 2015; 6: 18653–18663. https://doi.org/10.18632/oncotarget.4418.

[60] Liang JH, Gao R, Xia Y, Gale RP, Chen RZ, Yang YQ, *et al*. Prognostic impact of Epstein-Barr virus (EBV)-DNA copy number at diagnosis in chronic lymphocytic leukemia. Oncotarget. 2016; 7: 2135–2142. https://doi.org/10.18632/oncotarget.6281.

[61] Qiu J, Cosmopoulos K, Pegtel M, Hopmans E, Murray P, Middeldorp J, *et al*. A novel persistence associated EBV miRNA expression profile is disrupted in neoplasia. PLoS Pathogens. 2011; 7: e1002193. https://doi.org/10.1371/journal.ppat.1002193.

[62] Yang HJ, Huang TJ, Yang CF, Peng LX, Liu RY, Yang GD, *et al*. Comprehensive profiling of Epstein-Barr virus-encoded miRNA species associated with specific latency types in tumor cells. Virology Journal. 2013; 10: 314. https://doi.org/10.1186/1743-422X-10-314.

[63] Poling BC, Price AM, Luftig MA, Cullen BR. The Epstein-Barr virus miR-BHRF1 microRNAs regulate viral gene expression in cis. Virology. 2017; 512: 113–123. https://doi.org/10.1016/j.virol.2017.09.015.

[64] DiLillo DJ, Weinberg JB, Yoshizaki A, Horikawa M, Bryant JM, Iwata Y, *et al*. Chronic lymphocytic leukemia and regulatory B cells share IL-10 competence and immunosuppressive function. Leukemia. 2013; 27: 170–182. https://doi.org/10.1038/leu.2012.165.

[65] Mohr A, Renaudineau Y, Bagacean C, Pers JO, Jamin C, Bordron A. Regulatory B lymphocyte functions should be considered in chronic lymphocytic leukemia. Oncoimmunology. 2016; 5: e1132977. https://doi.org/10.1080/2162402X.2015.1132977.

[66] Manna A, Kellett T, Aulakh S, Lewis-Tuffin LJ, Dutta N, Knutson K, *et al*. Targeting CD38 is lethal to Breg-like chronic lymphocytic leukemia cells and Tregs, but restores CD8+ T-cell responses. Blood Advances. 2020; 4: 2143–2157. https://doi.org/10.1182/bloodadvances.2019001091.

[67] Cao Z, Leng P, Xu H, Li X. The regulating role of galectin-9 in immune cell populations. Frontiers in Pharmacology. 2024; 15: 1462061. https://doi.org/10.3389/fphar.2024.1462061.